Modeling Earth Systems and Environment
https://doi.org/10.1007/s40808-024-02020-4

ORIGINAL ARTICLE

Modelling the dynamics of Ebola disease transmission with optimal control analysis

Isaac Kwasi Adu[1] · Fredrick Asenso Wireko[2] · Sacrifice Nana-Kyere[4] · Ebenezer Appiagyei[5] · Mojeeb A. L.-Rahman E. L.-Nor Osman[6] · Joshua Kiddy K. Asamoah[2,3]

Received: 13 March 2024 / Accepted: 13 April 2024
© The Author(s), under exclusive licence to Springer Nature Switzerland AG 2024

Abstract

Ebola disease is a highly infectious and often deadly disease caused by the Ebola virus. Ebola can spread among humans through direct contact with the blood, secretions, organs, or other bodily fluids of infected people, as well as surfaces and materials contaminated with fluids of infected people. This article examines a non-linear mathematical model of Ebola, considering environmental contamination and safe burier. The boundedness, non-negativity, and well-posedness of the proposed model are obtained. The Ebola-free equilibrium, Ebola-present equilibrium and Ebola reproduction number ($\mathcal{R}_0$) are determined. A sensitivity analysis is conducted on the Ebola reproduction number to identify the factors that affect the output of $\mathcal{R}_0$. Furthermore, we found that the proposed Ebola model displays forward bifurcation, which means that Ebola spread can be suppressed by bringing the Ebola reproduction number down to unity. The numerical simulation of the proposed model without optimal control demonstrated that Ebola can be controlled by lowering the frequency of interaction with infectious people and contaminated environments, educating the public about Ebola reinfection, vaccinating recovered Ebola patients, and stepping up educational campaigns against funeral customs like bathing corpses. Based on these, we formulated an optimal control and a cost-effectiveness analysis was conducted on the model to establish the strategy or strategies that can be best used to control Ebola spread with a minimal cost. The study revealed that the most economical method involves personal protection, vaccination, and ensuring a secure burial.

Keywords Epidemic model · Basic Reproduction Number · Objective function · Existence of optimal control · Forward-Sweep Method

Mathematics Subject Classification 37C60 · 49M05

Introduction

Ebola Virus Disease (EVD) is a tropical disease transmitted from animals to humans (Troncoso 2015; Conrad et al. 2016). The mean death rate is 50% with a range between 25 – 90% in past occurrences. The primal occurrence of the disease was in the Democratic Republic of the Congo in the year 1976 and was given its name in commemoration of the neighbouring river called Ebola (Roca et al. 2015). In West Africa, the disease has so far recorded 28,646 cases with 11,323 deaths between December 26, 2013, and March 30, 2016, Team (2014) and Rosenke et al. (2016). Carriers of the disease exhibit symptoms such as fever, weakness, and diarrhoea. There are also bleeding complications which may occur in Ebola infectious people. EVD's incubation varies between two and twenty-one days. Infectious people

✉ Joshua Kiddy K. Asamoah
jkkasamoah@knust.edu.gh

[1] Department of Mathematical Sciences, Kumasi Technical University, Kumasi, Ghana

[2] Department of Mathematics, Kwame Nkrumah University of Science and Technology, Kumasi, Ghana

[3] Department of Mathematics, Saveetha School of Engineering SIMATS, Chennai, India

[4] Department of Mathematics, Valley View University, Oyibi, Ghana

[5] Department of Mathematics Education, Akenten Appiah-Menkah University of Skills Training and Entrepreneurial Development, Kumasi, Ghana

[6] Department of Mathematics and Computer Science, International University of Africa, Khartoum, Sudan

are unable to spread the disease until they show symptoms (Team 2014). It is believed that Fruit bats are the major carrier of the virus without being infected (Tulu et al. 2017; Jones et al. 2005). Humans, Apes and other mammals that are prone to Ebola virus (EV) infection are considered end hosts (Feldmann and Geisbert 2011).

The spread of Ebola starts via people's interaction with infectious animals (Roca et al. 2015; Bray et al. 2014). Once the first person contracts the disease, the person infects other individuals via direct interaction with the bodily fluids of dead victims of the disease. Other human fluids through which the disease can spread are faeces, and vomit (Roca et al. 2015). It is also believed that urine, saliva, breast milk, semen and sweat can contribute to the spread of the Ebola virus (Roca et al. 2015; Dowell et al. 1999). Transmission can also occur through contact with contaminated objects and surfaces with the Ebola virus. The Ebola virus can persist for several hours or days on contaminated surfaces. Funeral rites such as the washing of dead bodies are also contributing factors to the spread EVD (Troncoso 2015; Conrad et al. 2016; Dowell et al. 1999; Chan 2014).

Reinfection with EVD is considered a possibility because of partial immunity, a high viral load during a re-challenge, or a combination of both of these two factors. Empirical studies indicate that, after a few years of recovery, Ebola virus antibody potency reduces completely in some survivors (Wauquier et al. 2009; MacIntyre and Chughtai 2016). A recent report on a group of Guinean women indicates that they were not infected with Ebola despite repeated exposure to the virus, and only one of them had Ebola antibodies in the blood (MacIntyre and Chughtai 2016; Heffernan et al. 2005; Leroy et al. 2000). Furthermore, four (4) out of six (6) people who recovered from the Gulu strain of Sudan Ebola outbreak that appeared in the year 2000 in Uganda, tested positive for Ebola infection after 12 years of recovery (Lamunu et al. 2004; Sobarzo et al. 2013).

We now focus on some related mathematical models of EVD that have been previously published by other researchers. Many researchers who have conducted related studies on the spread of EVD outbreaks concentrate solely on the populace and the direct propagation of humans. Barely all the works on the dynamics of EVD outbreaks and its transmission are geared towards describing the classical settings (Berge et al. 2017). For instance, SI-model (Berge et al. 2017; Wang and Zhong 2015) SIR-model (Fisman et al. 2014; Rachah and Torres 2015), SEIR-model (Webb and Browne 2016; Legrand et al. 2007; Siettos et al. 2015), SEIRD-model (Chowell and Nishiura 2014; Ndanguza et al. 2013), SEIRHD-model (Zhang et al. 2022b; Gomes et al. 2014; Siriprapaiwan et al. 2018; Adu et al. 2023), where S, E, I, H, R and D denote the Susceptible, Exposed, Infectious, Hospitalized, Removed, and Dead/Deceased respectively. In addition to the above-mentioned compartment that was incorporated by researchers in their models, Imran et al. (2017), divided the Dead/Deceased (D) compartment into two distinct compartments. Namely; dead but not buried (F) and dead who are buried (R_D). Furthermore, Berge et al. (2017), incorporated the infection of EVD through a contaminated environment resulting from the virus's existence in the surroundings of the deceased Ebola victims in their *SIRPD* model, where P represents Ebola pathogens in the immediate environment.

One of the areas of mathematical modelling is to demonstrate how to optimally prevent the spread of disease and enable decision-making during an epidemic. For instance, Yusuf and Benyah (2012), presented a SIR model-based optimal control problem with potential control mechanisms that included treatment and vaccination. To reduce the cost of those preventive protocols, they investigated the best vaccination and treatment combinations.

Lashari and Zaman (2012) used optimal control analysis to examine some vector-borne infections like malaria, dengue fever, and the West Nile virus, that directly infects the host population. They applied various numerical methods to confirm the theoretical findings and verified the presence of the optimal problem. Seck et al. (2022), developed a model to study how Ebola spreads. They took into account the impact of different preventive strategies, including vaccination, public awareness campaigns, early identification campaigns, increased hygienic standards in hospitals, isolation of infected people, and geographic limitations. According to various operative limits, they developed an optimal control approach that envisages decreasing the number of Ebola cases. They also investigate the occurrence and distinctiveness of the optimal control.

Mhlanga (2019), employed a two-patch model to examine the EVD epidemic. They derived the threshold, the Ebola-Free and the Ebola-present equilibrium when the disease exists in the two sub-populations under particular circumstances. They included time-dependent controls in their suggested model. They also looked at the optimal control problem when the control system is an EVD epidemiological model with integrated awareness programs. In each patch, the control features correspond to the educational campaigns, with some controls being more efficient than others. To minimize the expenses associated with implementing the intervention while eradicating EVD in individual communities, we plan to explore how these control measures might be applied for a set period.

To evaluate the effectiveness of vaccines and the media in containing the spread of infectious diseases, a mathematical model of media awareness was put forth in Mondal et al. (2022) and modified into an optimal control. The media awareness control method was studied under three phenomena to offer a framework for public health to manage infectious diseases. To mitigate the coronavirus epidemic in India, Tiwari et al. (2021) looked at the combined effects of local awareness and media campaigns. The model was fitted to Indian data to estimate a few key parameters. The study found that the controls had an incomparable impact on the suggested mitigating methods. A mathematical model of media awareness was put forth in and revised as an ideal control to evaluate the role of vaccines and the media in containing the spread of infectious diseases. The media awareness control plan was looked at under three phenomena to offer a framework for public health to manage infectious diseases.

Mugabi et al. (2024) used mathematical model to study the behaviours of honeybees can reduce the probability of deformed wing virus outbreaks in Varroa destructor-infested colonies. Abidemi (2023) studied an Optimal cost-effective control of drug abuse by students: insight from mathematical modeling. A mathematical modelling of within-host Chikungunya virus dynamics with adaptive immune response was presented by Alade et al. (2023). LADT is used to analyse a numerical analysis with the SDIQR mathematical model of COVID-19 for Odisha's infected migrants. Analytical power series and LADT estimate dynamical variable solution profiles in the COVID-19 model in the work of Sahu and Jena (2023). The study conducted by Peter et al. (2022) focuses on the development and analysis of a deterministic mathematical model for the monkeypox virus. The requirements for both local and global asymptotic stability of disease-free and endemic equilibria are determined. Evidence indicates that the model experiences a backward bifurcation, in which the locally stable disease-free equilibrium coexists with an endemic equilibrium. The study conducted by Alla Hamou et al. (2024) introduced a mathematical model that incorporates the memory effect to simulate HIV transmission in a heterosexual community. The population is separated into two age groups: the young class, consisting of individuals aged 15–24, and the grown class, consisting of individuals aged 25 and above. The objective of categorising the population by age is to pinpoint the most susceptible group to the virus based on their sexual behaviour and generate precise forecasts on HIV transmission. Ahmad et al. (2024) developed an optimal control system that incorporated three tactics (public awareness campaign, post-exposure vaccination, and isolation) to identify the most effective combination for significantly reducing disease transmission or eliminating it. It was demonstrated that optimal control does exist, and we determined the requirements for optimality by applying Pontryagin's concept. Berge et al. (2017) presented a Susceptible, Infectious and Recovered (SIR) model which incorporates the eating of tainted wild game, practising of traditional funeral rites and contamination of the Ebola virus in the surrounding.

The current model extends the works of Berge et al. (2017) and Juga et al. (2021), by incorporating the Exposed compartment (E), Hospitalization compartment (H), and Safe burrier compartment (B). Furthermore, studies by Wauquier et al. (2009), MacIntyre and Chughtai (2016), Heffernan et al. (2005), Sobarzo et al. (2013) and Lamunu et al. (2004), indicates that Ebola antibodies reduce drastically in some survivors after a few years of recovery. Hence, the modification introduced in our analysis is that reinfection of Ebola virus disease after recovery is possible. Finally, we studied the optimal control version of the proposed EVD model using personal protection, vaccination, treatment and ensuring a secure burial with a comprehensive cost-effectiveness analysis.

The system of differential equations proposed by Juga et al. (2021) is as follows:

$$\begin{cases} \dfrac{dS}{dt} &= \pi - (\lambda + \mu)S, \\ \dfrac{dI}{dt} &= \lambda S - v_1 I, \\ \dfrac{dH}{dt} &= \sigma_2 - v_2 H, \\ \dfrac{dD}{dt} &= \sigma_3 I + \gamma_2 H - \rho D, \\ \dfrac{dP}{dt} &= \alpha_1 I + \alpha_2 D - \theta P, \end{cases} \tag{1}$$

the respective meaning of the various parameters can be found in (Juga et al. 2021).

The article is categorized as follows: "Ebola model presentation" contains the model formulation. In "Model analysis" we present the analysis of the model, thus, the Ebola-free equilibrium, the Ebola present equilibrium, Ebola reproduction number, $\mathcal{R}_0$, condition that leads to the occurrence of bifurcation in Ebola model, sensitivity analysis of the Ebola reproduction number, $\mathcal{R}_0$. In the "Method", we present the optimal control Ebola model. In the "Results" focuses on presenting the results of numerical analysis of the optimal control analysis and conducting efficiency and cost-effectiveness analysis. In "Discussion" we present the various discussion to the numerical simulation and cost-effectiveness analysis. The concluding remarks are given in "Conclusion".

Ebola model presentation

We formulate a non-linear *SEIHFDBR* mathematical model of Ebola virus disease that captures environmental contamination of Ebola virus pathogens and Ebola virus reinfection after recovery based on the model proposed by Juga et al. (2021). The total population $N(t)$, where t indicates time, is subdivided into eight(8) compartments. People who are prone to Ebola infection are referred as Susceptible and are denoted as $S(t)$. When the susceptible individuals are exposed to Ebola, they move to the exposed compartment at time t denoted as $E(t)$. After that, they progress to the infectious class (symptomatic) at time t denoted as $I(t)$. Ebola victims either go to the hospital at time t denoted as $H(t)$ or do not. The deceased Ebola victims without safe burier at time t, is denoted as $D(t)$. Those in the hospital have a greater chance of recovery from Ebola at time t denoted as $R(t)$. If they do not survive, they may be given a safe burier at time t denoted as $B(t)$. A traditional funeral may be performed for the deceased Ebola victims and other people may be infected through funeral practices like washing the dead Ebola victim during burial ceremonies. Deceased Ebola victims can still transmit the disease through the spreading of the virus pathogens in the surroundings. Ebola virus pathogens in the surroundings at time t, is denoted as $F(t)$. Interactions between $S(t) \leftarrow D(t)$, $S(t) \leftarrow F(t)$ and $S(t) \leftarrow H(t)\, S(t) \leftarrow I(t)$ result in new exposure, and that of $I(t) \rightarrow D(t)\, I(t) \rightarrow F(t)$, $H(t) \rightarrow D(t)$, $H(t) \rightarrow F(t)$, and $D(t) \rightarrow F(t)$ denote shedding of the virus. We developed the model based on the following presumptions: Ebola virus can be transmitted to other people when they are in contact with people infected in the compartment I, H and the environmental compartment, F. The deceased Ebola victims, D can still infect other people with the Ebola virus. There is no transmission of the Ebola virus when the safe burial of deceased Ebola victims is ensured. The infectious, hospitalized and deceased Ebola victims shed the virus around the environment at the rates ϕ, b, and β respectively. The rate at which the deceased Ebola victims are transferred from hospitals to their various homes for funeral rites and burial is y. Furthermore, the rate at which people get infected with Ebola virus disease is given by $\lambda = (\alpha_1 I + \alpha_2 H + \alpha_3 F + \alpha_4 D)S$, which is similar to Berge et al. (2017), where $\alpha_1, \alpha_2, \alpha_3$ and α_4 are the transmission rates of Ebola from infectious individuals, hospitalized individuals, environment, and dead Ebola victims respectively. The susceptible class is increased either by birth or immigration by a recruitment rate denoted as Ω. μ represents the natural death rate. The other parameters are described in Table 1. From the above description and the flow chart in Fig. 1 we have the following system of equations:

Table 1 Model parameters

Parameter	Meaning
Ω	Population growth rate
α_1	Contact rate of infectious human
α_2	Transmission rate of hospitalized Ebola infectious individuals
α_3	Transmission rate of Ebola from the surroundings
α_4	Transmission rate of deceased Ebola victims
μ	The natural death rate
κ_1	Rate at which Ebola virus decay in the surroundings
β	Rate at which the virus is shed by a deceased human in the surroundings
ϕ	Rate at which the virus is shed by Ebola-infected individuals
b	Rate at which the virus is shed by hospitalized Ebola victims
η	Rate at which infectious individuals are hospitalized
γ	Removed rate of infected individuals
ρ	Transmission coefficient from R to S(loss of immunity rate)
σ	Transfer rate from exposed to infectious class
κ_3	Safe burial rate
κ_2	Caring rate of deceased individuals
δ_1	Disease related death rate of Ebola-infected individuals
δ_2	Disease related death rate of hospitalized Ebola-infected individuals
y	Rate of transfer of deceased Ebola victims from hospitals for traditional burial
q	Transfer rate from D to B

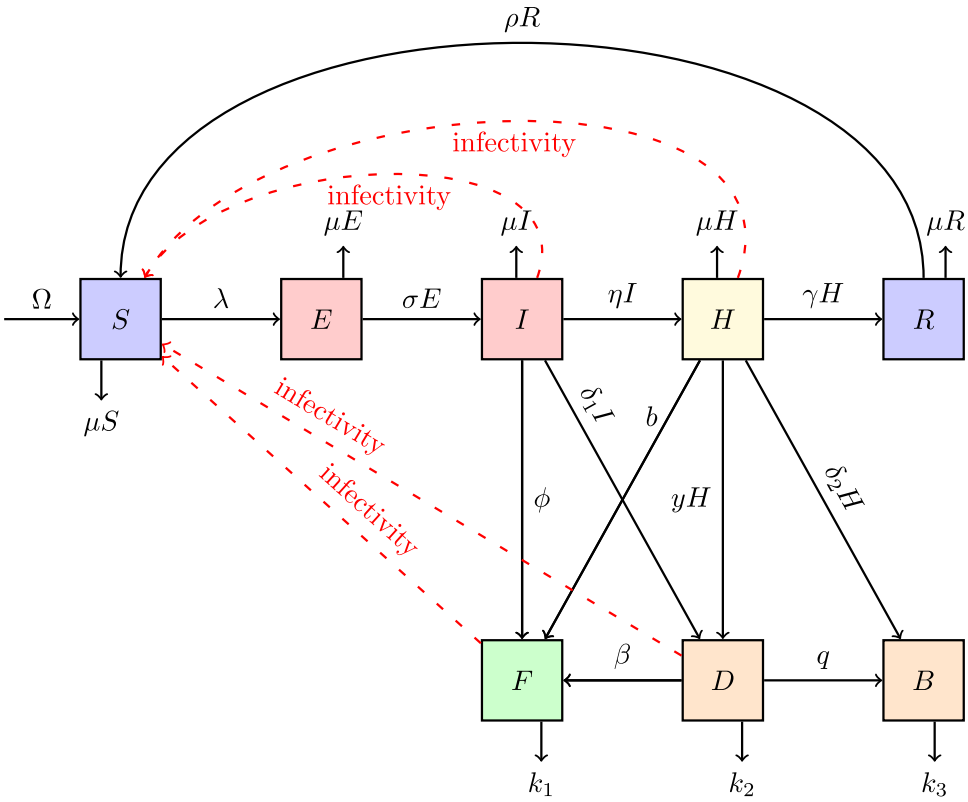

Fig. 1 Flowchart showing the transition between the model states

$$\begin{cases} \frac{dS}{dt} &= \Omega - (\alpha_1 I + \alpha_2 H + \alpha_3 F + \alpha_4 D)S - \mu S + \rho R, \\ \frac{dE}{dt} &= (\alpha_1 I + \alpha_2 H + \alpha_3 F + \alpha_4 D)S - (\mu + \sigma)E, \\ \frac{dI}{dt} &= \sigma E - (\mu + \delta_1 + \eta)I, \\ \frac{dH}{dt} &= \eta I - (\mu + \gamma + \delta_2 + y)H, \\ \frac{dF}{dt} &= \phi I - \kappa_1 F + \beta D + bH, \\ \frac{dD}{dt} &= \delta_1 I - (q + \kappa_2)D + yH, \\ \frac{dB}{dt} &= \delta_2 H + qD - \kappa_3 B, \\ \frac{dR}{dt} &= \gamma H - (\mu + \rho)R, \end{cases} \tag{2}$$

with initial conditions

$$\begin{cases} S(0) = S_0 > 0,\ E(0) = E_0 \geq 0,\ I(0) = I_0 \geq 0, H(0) = H_0 \geq 0, \\ F(0) = F_0 \geq 0, D(0) = D_0 \geq 0, B(0) = B_0 \geq 0, R(0) = R_0 \geq 0. \end{cases} \tag{3}$$

Well-posedness of the model

For biological reasons, we study the positive and constrained nature of our model's solutions. From Eq. (2), $\frac{dS}{dt}$ can be written as,

$$\frac{dS}{dt} = \Omega - (\mu + \theta)S + \rho R, \tag{4}$$

where $\theta = \beta_1(\alpha_1 I + \alpha_2 H + \alpha_3 F + \alpha_4 D)$. It follows that,

$$\begin{aligned} S(t) &= S(0)e^{-(\mu+\theta)t} + e^{-(\mu+\theta)t}\rho \int_0^t R(\tau)e^{(\mu+\theta)\tau}d\tau, \\ &= e^{-(\mu+\theta)t}\left[S(0) + \rho \int_0^t R(\tau)e^{(\mu+\theta)\tau}d\tau\right]. \end{aligned} \tag{5}$$

From the above solution for $S(t)$, it implies that $\frac{dS}{dt}|_{t=t_0} \geq 0$, provided $S(t_0) = 0$. This ensures that the state variable S stays non-negative in the model system (2). With the same idea for the remaining state variables, model system (4) is rewritten in the form

$$\frac{dQ}{dt} = XQ(t) + C(t), \tag{6}$$

where,

$$Q(t) = \begin{bmatrix} E \\ I \\ H \\ F \\ D \\ B \\ R \end{bmatrix},$$

$$x(t) = \begin{bmatrix} -(\mu+\sigma) & \alpha_1 S & \alpha_2 S & \alpha_3 S & \alpha_4 S & 0 & 0 \\ \sigma & -(\mu+\delta_1+\eta) & 0 & 0 & 0 & 0 & 0 \\ 0 & \eta & -(\gamma+\mu+\delta_2+y) & 0 & 0 & 0 & 0 \\ 0 & \phi & b & -\kappa_1 & \beta & 0 & 0 \\ 0 & \delta_1 & y & 0 & -(q+\kappa_2) & 0 & 0 \\ 0 & 0 & \delta_2 & 0 & q & -\kappa_3 & 0 \\ 0 & 0 & \gamma & 0 & 0 & 0 & -(\mu+\rho) \end{bmatrix}, \tag{7}$$

$$C(t) = \begin{bmatrix} 0 \\ 0 \\ 0 \\ 0 \\ 0 \\ 0 \\ 0 \end{bmatrix}.$$

Hence, matrix $x(t)$ is a Metzler matrix, because of its non-negative off-diagonal components. This is in line with our already established assumption that S is non-negative. This means that Eq. (6) is a monotone system (Berge et al. 2017). Adding the first, second, third, fourth and eight equations of system (2) together, we obtained the conservation law:

$$\frac{dM}{dt} = \Omega - \mu M - \delta_1 I - \delta_2 H - yH, \tag{8}$$

where, $M = S + E + I + H + R$ is the entire active human population, i.e. individuals who are still living. We consider additional assumption that the barrier rates κ_2 and κ_3 are either lower or same as total death $\mu + \delta_1$ and $\mu + \delta_2$. If this requirement is not fulfilled, the dead person vanishes completely from the community such that considering compartments B and D in this model is not relevant. Equation (8) leads to the conclusion that the model (2) is bounded. Thus,

$$\limsup_{t\to\infty} M(t) \le \frac{\Omega}{\mu}. \tag{9}$$

Our next step is to assert and demonstrate that system (2) solutions are bounded.

Proposition 1 *Suppose that system* (2) *preliminary requirements have been met. Equation* (2) *satisfy*

$$M(0) \le M_n, H(0) \le H_n, F(0) \le F_n, D(0) \le D_n, \tag{10}$$

where

$$\begin{aligned} M_n &= \frac{\Omega}{\mu},\ H_n = \frac{\eta\Omega}{(\mu+\gamma+\delta_2+y)\mu}, \\ F_n &= \frac{\phi\Omega(\kappa_2+q)(\mu+\gamma+\delta_2+y) + \beta[(\delta_1\Omega(\mu+\gamma+\delta_2+y) + y\eta\Omega) + (\kappa_2+q)b\eta\Omega]}{(\kappa_2+q)(\mu+\gamma+\delta_2+y)\mu}, \\ D_n &= \frac{\delta_1\eta(\mu+\gamma+\delta_2+y) + y\eta\Omega}{(\kappa_2+q)(\mu+\gamma+\delta_2+y)\mu}. \end{aligned} \tag{11}$$

Therefore, the result fulfils the following constraints when it occurs on an interval P. Thus,

$$P = \left\{M(t) \le M_n, H(t) \le H_n, F(t) \le F_n, D(t) \le D_n\right\}. \quad (12)$$

Proof Because $I(t) \ge 0$, Eq. (8) reminds us of

$$\frac{dM(t)}{dt} \le \Omega - \mu M. \quad (13)$$

Applying Gronwall's inequality gives,

$$M(t) \le \frac{\Omega}{\mu} + \left(M(0) - \frac{\Omega}{\mu}\right)e^{-\mu t}, \quad (14)$$

for which $M(t) \le M_n$, whenever $M(0) \le M_n$. The result is that, $I(t) \le N_n$. Substituting it into the sixth equation of (2), we obtain

$$\frac{dD(t)}{dt} \le \delta_2 M_n - (q + \kappa_2)D + yH, \quad (15)$$

where the other use of grownwell inequality results in $D(t) \le D_n$ if $D(0) \le D_n$ and $H(0) \le H_n$. The boundedness of $F(t)$ can be proved similarly. Hence, the biologically acceptable area of the model (2) is

$$\begin{aligned}
\Gamma &= \left\{ S(t), E(t), I(t), H(t), R(t), F(t), D(t), B(t)) \in \mathcal{R}_+^8, \right. \\
M_n &= \frac{\Omega}{\mu}, \; H_n = \frac{\eta\Omega}{(\mu+\gamma+\delta_2+y)\mu}, \\
F_n &= \frac{\phi\Omega(\kappa_2+q)(\mu+\gamma+\delta_2+y) + \beta[(\delta_1\Omega(\mu+\gamma+\delta_2+y) + y\eta\Omega) + (\kappa_2+q)b\eta\Omega]}{(\kappa_2+q)(\mu+\gamma+\delta_2+y)\mu}, \\
D_n &= \left. \frac{\delta_1\eta(\mu+\gamma+\delta_2+y) + y\eta\Omega}{(\kappa_2+q)(\mu+\gamma+\delta_2+y)\mu} \right\}.
\end{aligned} \quad (16)$$

□

Model analysis

This section discusses the existence and stability of the system (2) around different equilibria. The System (2) has an Ebola-free equilibrium (EFE):

$$E_0 = \left(\frac{\Omega}{\mu}, 0, 0, 0, 0, 0, 0, 0\right). \quad (17)$$

The basic(Ebola) reproduction number

The mean number of secondary cases that a typical infectious individual would generate in a population that is fully susceptible is known as the basic reproduction number. Reproduction number offers a threshold that is essential in determining whether the illness spreads across the population or eventually disappears (Khajanchi et al. 2021; Das et al. 2020a; Khajanchi et al. 2018). The subsection considers the generally used method, the next generation matrix (Siriprapaiwan et al. 2018; Brauer et al. 2012; Sharma and Samanta 2017; Das et al. 2020b) to derive the $\mathcal{R}_0$ for model system 2. We denote $X = (E, I, H, F, D)^T$, thus, model (2) may be expressed as $\frac{dX}{dt} = \mathcal{F}(X) - \mathcal{V}(X)$.

$$\begin{aligned}
\mathcal{F}(X) &= \begin{bmatrix} (\alpha_1 I + \alpha_2 H + \alpha_3 F + \alpha_4 D)S \\ 0 \\ 0 \\ 0 \\ 0 \end{bmatrix}, \\
\mathcal{V}(X) &= \begin{bmatrix} (\mu+\sigma)E \\ -\sigma E + (\mu + \delta_1 + \eta)I \\ -\eta I + (\mu + \gamma + \delta_2 + y)H \\ -\phi I + \kappa_1 F - \beta D - bH \\ -\delta_1 I + (q + \kappa_2)D - yH \end{bmatrix}.
\end{aligned} \quad (18)$$

The Jacobian matrices of $\mathcal{F}(X)$ and $\mathcal{V}(X)$ at E_0 are respectively

$$F = \begin{bmatrix} 0 & \alpha_1 S & \alpha_2 S & \alpha_3 S & \alpha_4 S \\ 0 & 0 & 0 & 0 & 0 \\ 0 & 0 & 0 & 0 & 0 \\ 0 & 0 & 0 & 0 & 0 \\ 0 & 0 & 0 & 0 & 0 \end{bmatrix}, \; V = \begin{bmatrix} D_1 & 0 & 0 & 0 & 0 \\ -\sigma & D_2 & 0 & 0 & 0 \\ 0 & -\eta & D_3 & 0 & 0 \\ 0 & -\phi & -b & \kappa_1 & -\beta \\ 0 & -D_4 & -y & 0 & D_5 \end{bmatrix}. \quad (19)$$

Thus we compute FV^1 as

$$FV^{-1} = \begin{bmatrix} \kappa_{11} & \kappa_{12} & \kappa_{13} & \kappa_{14} & \kappa_{15} \\ 0 & 0 & 0 & 0 & 0 \\ 0 & 0 & 0 & 0 & 0 \\ 0 & 0 & 0 & 0 & 0 \\ 0 & 0 & 0 & 0 & 0 \end{bmatrix}, \quad (20)$$

where,

$$\kappa_{11} = \frac{\sigma\eta\Omega}{D_1D_2\mu}[\frac{\alpha_1}{\eta} + \frac{\alpha_2}{D_3} + \frac{\alpha_3 b}{D_3\kappa_1} + \frac{\alpha_4 y}{D_3D_4}], \tag{21}$$

$$\kappa_{12} = \frac{\alpha_1\Omega}{\mu D_2} + \frac{\alpha_2\eta\Omega}{\mu D_2D_3} + \frac{\alpha_3\eta(bD_4+\beta y)\Omega}{\mu D_2D_3D_4\kappa_1} + \frac{\alpha_4\eta\Omega y}{\mu D_2D_3D_4}, \tag{22}$$

$$\kappa_{13} = \frac{\alpha_2\Omega}{\mu D_2} + \frac{\alpha_3(bD_4+\beta y)\Omega}{\mu D_3D_4\kappa_1} + \frac{\alpha_4\Omega y}{\mu D_3D_4}, \tag{23}$$

$$\kappa_{14} = \frac{\alpha_3\Omega}{\mu\kappa_1}, \tag{24}$$

$$\kappa_{15} = \frac{\alpha_3\beta\Omega}{\mu D_4\kappa_1} + \frac{\alpha_4\Omega}{\mu D_4}, \tag{25}$$

with $D_1 = \mu+\sigma, D_2 = \mu+\delta_1+\eta, D_3 = \mu+\gamma+\delta_2+y,\ D_4 = q+\kappa_2$.

Finally, the Ebola reproduction number is given as,

$$\mathcal{R}_0 = g(FV^{-1}) = \frac{\sigma\eta\Omega}{D_1D_2\mu}\left[\frac{\alpha_1}{\eta} + \frac{\alpha_2}{D_3} + \frac{\alpha_3 b}{D_3\kappa_1} + \frac{\alpha_4 y}{D_3D_4}\right]. \tag{26}$$

Ebola-present equilibrium (EPE)

The Ebola-present equilibrium is given as $E_1(S^*, E^*, I^*, H^*, F^*, D^*, B^*, R^*)$, where,

$$\begin{cases} S^* = \dfrac{\Omega}{\mathcal{R}_0}, \\ B^* = \dfrac{\delta_2 H^* + qD^*}{k_3}, \\ I^* = \dfrac{\sigma E^*}{(\mu+\delta_1+\eta)}, \\ H^* = \dfrac{\eta\sigma E^*}{(\mu+\delta_1+\eta)(\mu+\gamma+\delta_2+y)}, \\ D^* = \dfrac{\delta_1 I^* + yH^*}{(q+k_2)}, \\ F^* = \dfrac{\phi I^* + \beta D^* + bH^*}{k_1}, \\ R^* = \dfrac{\gamma\eta\sigma E^*}{(\mu+p)(\mu+\delta_1+\eta)(\mu+\gamma+\delta_2+y)}, \\ E^* = \dfrac{(q+k_2)(\mu+\delta_1+\eta)(\mu+\gamma+\delta_2+y)(\mathcal{R}_0-1)}{\mathcal{R}_0(\mu+\rho)\left[(q+k_2)y_0 + \sigma\delta_1(\mu+\gamma+\delta_2+y)\left(\alpha_3\beta+\alpha_4+y\eta\right)\right]}, \end{cases} \tag{27}$$

where, $y_0 = \left(\alpha_1\sigma(\mu+\gamma+\delta_2+y) + \alpha_2\eta\sigma + \alpha_3 b\eta\sigma\right)$. From E^* it can be noticed that the Ebola-present equilibrium exits (positive) when the Ebola reproduction number is greater than a unity.

Bifurcation analysis

The Sect. (3.3) employs the theory of centre manifold as explained in the studies of Carlos Castillo-Chavez and Song (Castillo-Chavez and Song 2004), and B. Buonomo and D. Lacitignola (Buonomo and Lacitignola 2010) to the Ebola model (2) by considering the transfer rate α_1 as the bifurcation parameter, so that, $\mathcal{R}_0 = 1$ if and only if

$$\alpha_1 = \alpha_1^* = \frac{D_1D_2D_3D_4k_1\mu - \sigma\eta\Omega\left(\alpha_2D_4k_1 + \alpha_3D_4b + \alpha_4k_1y\right)}{\sigma\Omega k_1D_3D_4}, \tag{28}$$

where D_1, D_2, D_3 and D_4 have their usual meanings. We set $x_1 = S,\ x_2 = E,\ x_3 = I,\ x_4 = H,\ x_5 = F,\ x_6 = D,\ x_7 = B,\ x_8 = R$. System (2) becomes

$$\begin{aligned}
\frac{dx_1}{dt} &= \Omega - (\alpha_1 x_3 + \alpha_2 x_4 + \alpha_3 x_5 \\
&\quad + \alpha_4 x_6)x_1 - \mu x_1 + \rho x_8 = f_1, \\
\frac{dx_2}{dt} &= (\alpha_1 x_3 + \alpha_2 x_4 + \alpha_3 x_5 \\
&\quad + \alpha_4 x_6)x_1 - (\mu + \sigma)x_2 = f_2, \\
\frac{dx_3}{dt} &= \sigma x_2 - (\mu + \delta_1 + \eta)x_3 = f_3, \\
\frac{dx_4}{dt} &= \eta x_3 - (y + \mu + \delta_2 + \gamma)x_4 = f_4, \\
\frac{dx_5}{dt} &= \phi x_3 - k_1 x_5 + \beta x_6 + b x_4 = f_5, \\
\frac{dx_6}{dt} &= \delta_1 x_3 - (q + k_2)x_6 + y x_4 = f_6, \\
\frac{dx_7}{dt} &= \delta_2 x_4 - k_3 x_7 + q x_6 = f_7, \\
\frac{dx_8}{dt} &= \gamma x_4 - (\mu + \rho)x_8 = f_8.
\end{aligned} \tag{29}$$

We know that the Ebola-free equilibrium of the model (1) is given by $[x_1^* = \frac{\Omega}{\mu}, x_2^* = 0, x_3^* = 0, x_4^* = 0, x_5^* = 0, x_6^* = 0, x_7^* = 0, x_8^* = 0]$. The linearization of system (29) around the Ebola-free equilibrium evaluated at $\alpha_1 = \alpha_1^*$ is given by

$$V(E^*) = \begin{pmatrix}
-\mu & 0 & -z_1 & -z_2 & -z_3 & -z_4 & 0 & \rho \\
0 & -D_1 & z_1 & z_2 & z_3 & z_4 & 0 & 0 \\
0 & \sigma & -D_2 & 0 & 0 & 0 & 0 & 0 \\
0 & 0 & \eta & -D_3 & 0 & 0 & 0 & 0 \\
0 & 0 & \phi & b & -k_1 & B & 0 & 0 \\
0 & 0 & \delta_1 & y & 0 & -D_4 & 0 & 0 \\
0 & 0 & 0 & z_5 & 0 & 0 & -k_3 & 0 \\
0 & 0 & 0 & \gamma & 0 & 0 & 0 & -z_6
\end{pmatrix}, \tag{30}$$

The matrix (30) has a simple eigenvalue, with the remaining eigenvalues which have negative real parts. Therefore, the central manifold theorem (Castillo-Chavez and Song 2004) can be used. Therefore, we have to compute the values of a and b given by

$$\mathbf{a} = \sum_{k,i,j=1}^{n} \frac{v_k w_i w_j \partial^2 f_k(\alpha_1^*, 0)}{\partial x_i \partial x_j}, \tag{31}$$

and

$$\mathbf{b} = \sum_{k,i,j=1}^{n} \frac{v_k w_i \partial^2 f_k(\alpha_1^*, 0)}{\partial x_i \eta_1}. \tag{32}$$

We begin this by computing W and V given as $W = [w_1, w_2, w_3, w_4, w_5, w_6, w_7, w_8]^T$ and $V = [v_1, v_2, v_3, v_4, v_5, v_6, v_7, v_8]^T$ respectively. We obtain $w_1 = \frac{\sigma\eta\rho\gamma - (-(\mu+\rho))(\sigma+\mu)(\mu+\delta_1+\eta)(\gamma+\mu+\delta_2+y)}{\sigma\eta\mu(-(\mu+\rho))}$,
$w_2 = \frac{(\mu+\delta_1+\eta)(\gamma+\mu+\delta_2+y)}{\sigma\eta}$, $w_3 = \frac{(\gamma+\mu+\delta_2+y)}{\eta}$,
$w_4 = 1$, $w_5 = \frac{\phi(q+k_1)(\gamma+\mu+\delta_2+y)+b\eta(q+k_1)+\beta(\gamma+\mu+\delta_2+y)\delta_1+y\eta)}{k_1\eta(q+k_1)}$,
$w_6 = \frac{\delta_1(\gamma+\mu+\delta_2+y)+y\eta}{\eta(q+k_1)}, w_7 = -\frac{\delta_2}{k_3}, w_8 = \frac{\gamma}{-(\mu+rho)}$.
and $v_1 = 0$, $v_2 = 1$, $v_3 = \frac{(\sigma+\mu)}{\sigma}$,
$v_4 = \frac{b\alpha_3\Omega(q+k_1)+y(\alpha_4\Omega k_1+\beta\alpha_3\Omega)-\alpha_2\Omega(q+k_1)k_1}{\mu k_1(\gamma+\mu+\delta_2+y)(q+k_1)}$,
$v_5 = \frac{\alpha_3\Omega}{k_1\mu}$, $v_6 = \frac{\alpha_4\Omega k_1+\beta\alpha_3\Omega}{\mu k_1(q+k_1)}$, $v_7 = 0$, $v_8 = 0$. Next, we perform the computations of a and b. From system (29), all the associated partial derivatives of $F = (f_1, f_2, f_3, f_4, f_5, f_6, f_7, f_8)^T$ in (29) are zero at the Ebola-free equilibrium except the following
$\frac{\partial^2 f_1}{\partial x_1 \partial x_3} = \frac{\partial^2 f_1}{\partial x_3 \partial x_1} = -\alpha_1^*, \frac{\partial^2 f_1}{\partial x_1 \partial x_4} = \frac{\partial^2 f_1}{\partial x_4 \partial x_1} = -\alpha_2,$
$\frac{\partial^2 f_1}{\partial x_1 \partial x_5} = \frac{\partial^2 f_1}{\partial x_5 \partial x_1} = -\alpha_3, \frac{\partial^2 f_1}{\partial x_1 \partial x_6} = \frac{\partial^2 f_1}{\partial x_6 \partial x_1} = \alpha_2,$
$\frac{\partial^2 f_2}{\partial x_1 \partial x_3} = \frac{\partial^2 f_2}{\partial x_3 \partial x_1} = \alpha_1^*, \frac{\partial^2 f_2}{\partial x_1 \partial x_4} = \frac{\partial^2 f_2}{\partial x_4 \partial x_1} = \alpha_2,$
$\frac{\partial^2 f_2}{\partial x_1 \partial x_5} = \frac{\partial^2 f_2}{\partial x_5 \partial x_1} = \alpha_3, \frac{\partial^2 f_2}{\partial x_1 \partial x_6} = \frac{\partial^2 f_2}{\partial x_6 \partial x_1} = \alpha_2,$
$\frac{\partial^2 f_2}{\partial x_3 \partial \alpha_1^*} = \frac{\partial^2 f_2}{\partial \alpha_1^* \partial x_3} = \frac{\Omega}{\mu}$. Substituting the above expressions into equation a and b, it follows that

$$\begin{aligned}
a &= 2v_2 w_1 (w_3 \alpha_1^* + w_4 \alpha_2 + w_5 \alpha_3 + w_6 \alpha_4). \\
a &= \left(\frac{2\rho\gamma}{\mu(-(\mu+\rho))} - \frac{2(\mu+\sigma)(\mu+\delta_1+\eta)(\gamma+\delta_2+\mu+y)}{\sigma\eta\mu} \right) \\
&\quad \left[(\gamma+\delta_2+\mu+y) \left(\frac{(\alpha_1^* k_1 + \alpha_3\phi)(q+k_1) + (\alpha_4 k_1 + \beta)\delta_1}{k_1\eta(q+k_1)} \right) \right. \\
&\quad \left. + \frac{(b\eta + \alpha_2 k_1 \eta)(q+k_1) + \beta\eta y}{k_1\eta(q+k_1)} \right], \\
b &= \frac{\Omega(\gamma+\delta_2+\mu+y)}{\eta\mu} > 0.
\end{aligned}$$

It can be seen that the computation of b is positive. The sign of the coefficients of a and b guarantees the model dynamics at the EFE for α_1^*. It follows from the results given by Chen et al. (2016); Buonomo and Lacitignola (2010);

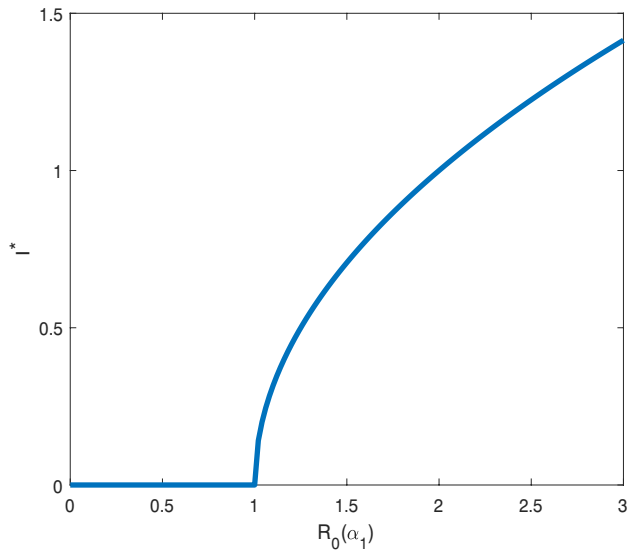

Fig. 2 Simulation of model (2) as a function of α_1 illustrating occurrence of forward bifurcation

Table 2 Sensitivity indices computation of $\mathcal{R}_0$

Parameter	Sensitivity index	Parameter	Sensitivity index
Ω	1	δ_1	−0.6399
η	0.1352	δ_2	−0.0591
σ	0.8962	γ	−0.0084
α_1	0.4995	q	−0.3095
α_2	0.0102	k_2	−0.0051
α_3	0.3614	y	−0.0314
α_4	0.1289		
μ	− 1.9780		

Castillo-Chavez and Song (2004), that model 2 undergoes backward bifurcation if

$$\frac{2\rho\gamma}{\mu(-(\mu+\rho))} > \frac{2(\mu+\sigma)(\mu+\delta_1+\eta)(\gamma+\delta_2+\mu+y)}{\sigma\eta\mu}, \quad (33)$$

so that $a > 0$ and $b > 0$. also, model 2 undergoes forward bifurcation if

$$\frac{2\rho\gamma}{\mu(-(\mu+\rho))} < \frac{2(\mu+\sigma)(\mu+\delta_1+\eta)(\gamma+\delta_2+\mu+y)}{\sigma\eta\mu}. \quad (34)$$

According to our analysis above, it can be seen that $\mathcal{R}_0 < 1$ can guarantee the EFE's global stability. The presence of forward bifurcation shows that Ebola can be eliminated by decreasing the basic reproduction ratio to a value of less than one. Also, since the bifurcation is forward, it implies that the Ebola-present equilibrium point does not coexist with the Ebola-free equilibrium. We therefore establish that the model is globally stable. Figure 2 below indicated the bifurcation diagram of model (2).

Sensitivity indices computation of $\mathcal{R}_0$

Considering the study of Chitnis et al. (2008), we carry out sensitivity indices computation of $\mathcal{R}_0$ with respect to the independent parameters of the $\mathcal{R}_0$ using Eq. (26). We are very much concerned with the parameter values that influence the reproduction number significantly because they are those parameters that need to be considered during intervention strategies. Hence, using the normalized forward sensitivity index of $\mathcal{R}_0$ with respect to σ, the computed indices are given in Table 2

$$\chi_{\sigma}^{\mathcal{R}_0} = \frac{\partial\mathcal{R}_0}{\partial\sigma}\frac{\sigma}{\mathcal{R}_0}, \quad (35)$$

Parameters whose sensitivity indices are negatives reduce the value of $\mathcal{R}_0$, and those positive parameters increase the $\mathcal{R}_0$ value with an increase in their values. The parameters with the most sensitive indices in this model are Ω, σ, δ_1, and μ. For example, a rise or decline in the value of σ by 10%, will cause a hike or lower the value of the $\mathcal{R}_0$ by 8.962%. In a similar manner, increasing or decreasing the value of Ω by 10% increases or decreases the value of $\mathcal{R}_0$ by 10%. Also, increasing or decreasing the value of δ_1 and μ by 10% increases or decreases the value of $\mathcal{R}_0$ by 6.399% and 19.780% respectively.

Figure 3, shows the contour graphs in support of the sensitiveness of some key parameters in Table 3. It is noticed that as σ, η, ϕ,α_1 and α_4 increases the number of Ebola infections increases, whiles an increase κ_2 decreases the number of Ebola infections. Figure 4, shows the 3D graphs in support of the sensitiveness of some key parameters in Table 3. It is noticed in Fig. 4a that κ_2 and q are inversely proportional to the Ebola reproduction number. Thus, an increase in κ_2 and q reduces the value of R_0. Also, α_1, σ, α_4 and η, are directly proportional to the $\mathcal{R}_0$. An increase in any of these parameters increases the value of $\mathcal{R}_0$. This implies that when σ, α_1, α_4, and η, increases the number of Ebola infections increases, whiles an increase q, and γ decreases the number of Ebola infections.

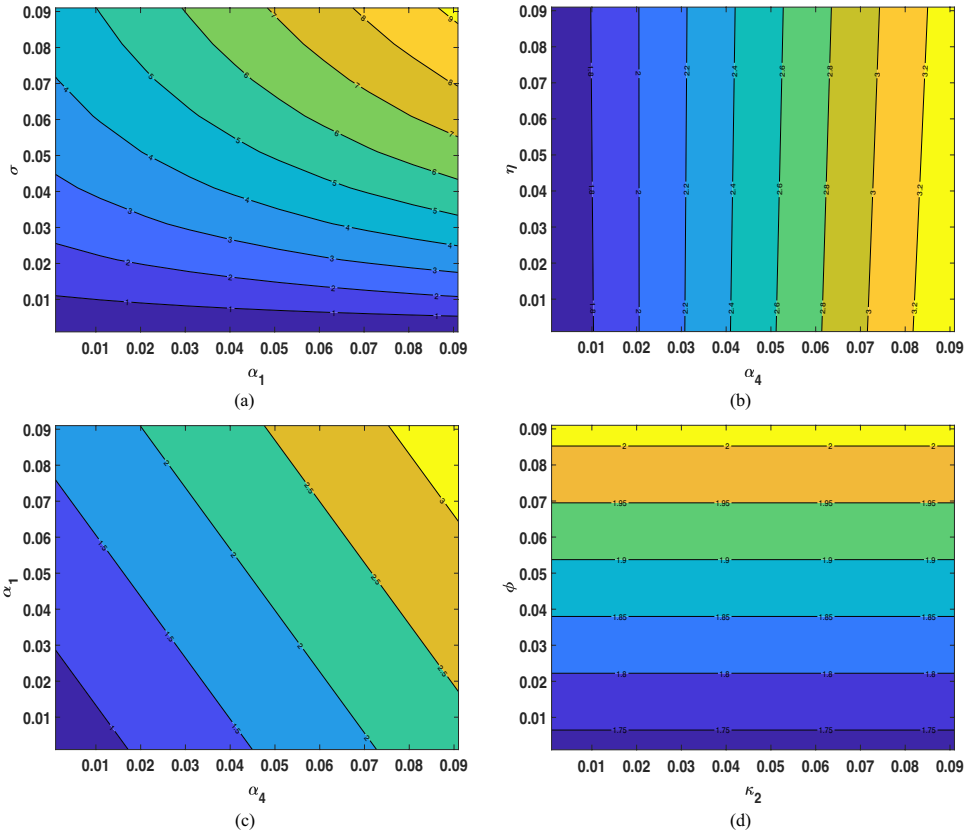

Fig. 3 Contour plot of α_1 and σ in Fig. 3b, α_4 and η, Fig. 3c, α_4 and α_1 and finally, Fig. 3d κ_2 and ϕ using values in Table 3

Table 3 Ebola parameter values and source

Parameter	Value	Source	Parameter	Value	Source
Ω	10	Takaidza et al. (2017)	η	0.15	Edward et al. (2017)
α_1	0.09	Ahmad et al. (2016)	γ	0.0356	Takaidza et al. (2017)
α_2	0.007	Xia et al. (2015)	ρ	0.00200	Edith et al. (2020)
α_3	0.009	(?)	σ	0.01	Assumed
α_4	0.0125	Xia et al. (2015)	κ_3	0.009	Juga et al. (2021)
μ	0.086	Takaidza et al. (2017)	κ_2	0.009	Juga et al. (2021)
κ_1	0.03	Berge et al. (2017)	δ_1	0.9000	Berge et al. (2017)
β	0.06	Juga et al. (2021)	δ_2	0.2500	Ahmad et al. (2016)
ϕ	0.04	Berge et al. (2017)	b	0.2500	Berge et al. (2017)
y	0.2	Juga et al. (2021)	q	0.55	Edward et al. (2017)

Method

Optimal Ebola control model

Here, as in the studies of Khajanchi and Ghosh (2015); Das et al. (2020b); Nana-Kyere et al. (2022); Zhang et al. (2022a); Asamoah et al. (2020); Mabotsa et al. (2022), we employ optimal control theory to determine controls for the Ebola model (2) to prevent the spreading of the epidemic and provide direction for public health. Thus, the non-control model (2) is modified based on the sensitivity analysis by adding time-dependent control of personal protection, $u_1(t)$, vaccination of the susceptible, $u_2(t)$, treatment of the infected individuals, $u_3(t)$, and ensuring a secure burial, $u_4(t)$. Hence, the newly formulated control model becomes:

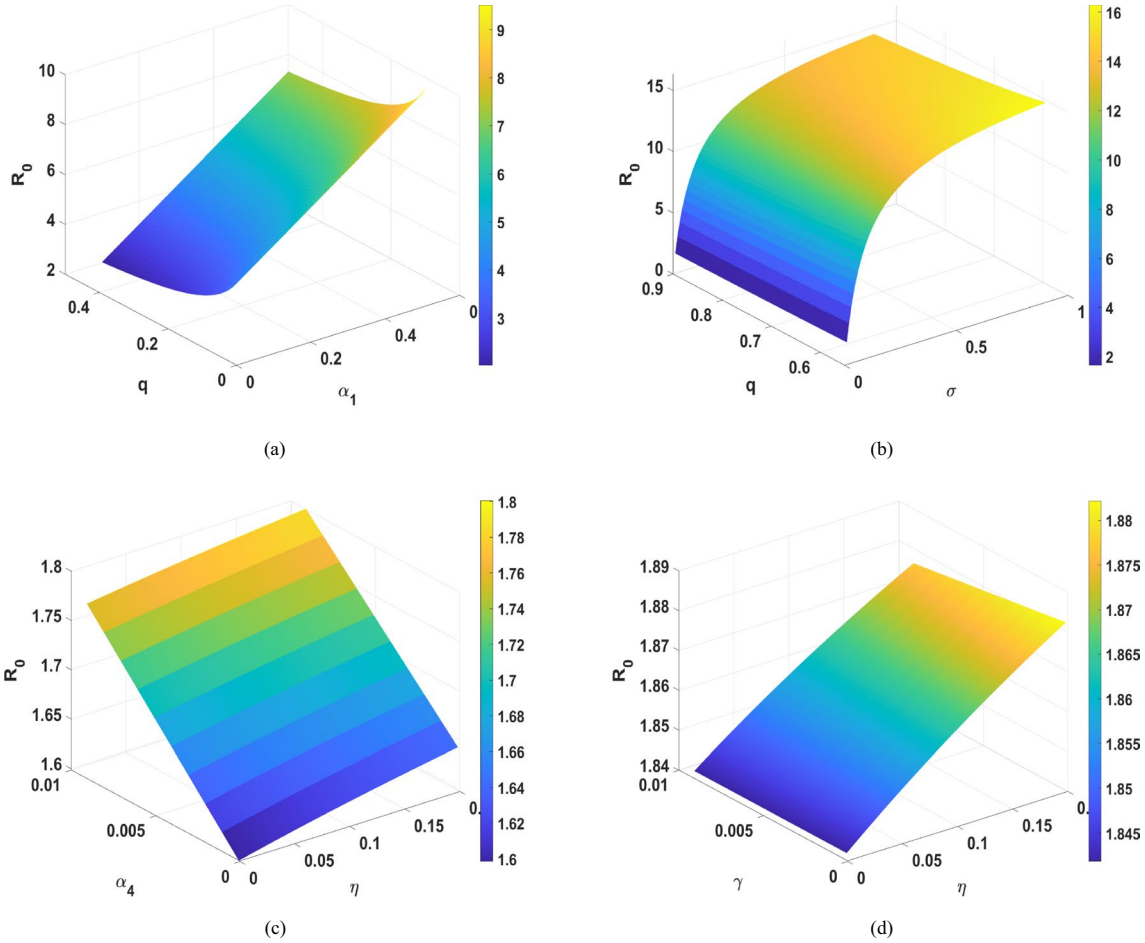

Fig. 4 Sensitivity plot of $\mathcal{R}_0$ in terms $\sigma, q, \eta, \alpha_1, \alpha_4$ and γ using values in Table 3

$$
\begin{cases}
\frac{dS}{dt} &= \Omega - (1-u_1)(\alpha_1 I + \alpha_2 H + \alpha_3 F + \alpha_4 D)S - \mu S + \rho R - u_2 S,\\
\frac{dE}{dt} &= (1-u_1)(\alpha_1 I + \alpha_2 H + \alpha_3 F + \alpha_4 D)S - (\mu+\sigma)E,\\
\frac{dI}{dt} &= \sigma E - (\mu + \delta_1 + \eta)I,\\
\frac{dH}{dt} &= \eta I - (\mu + \delta_2 + y + u_3)H,\\
\frac{dF}{dt} &= \phi I - \kappa_1 F + \beta D + bH,\\
\frac{dD}{dt} &= \delta_1 I - (u_4 + \kappa_2)D + yH,\\
\frac{dB}{dt} &= \delta_2 H - \kappa_3 B + u_4 D,\\
\frac{dR}{dt} &= u_3 H - (\mu + \rho)R + u_2 S.
\end{cases}
\tag{36}
$$

Model system (2) identified controls $u_1, u_2,\ u_3$ and u_4 with their respective meaning explicitly given in the formulation of the control model. The controls $\sum_{i=1}^{4} u_i$ that are in association with the state variables are bounded and Lebesgue measurable, with

$$
\begin{aligned}
\mathcal{J} = \{ & u(t) = u_i \in \mathcal{U}, i = 1, \ldots, 4, \text{with} \\
& 0 \le u(i) \le 1,\ t \in [0, T] \}.
\end{aligned}
\tag{37}
$$

With this in mind, our primary objective for the state (36) is to minimize $\mathcal{J}$ given by

$$
\begin{aligned}
\mathcal{J} = \int_0^t & [A_0 E + A_1 I + A_2 H + A_3 F + A_4 D \\
& + \frac{1}{2}(C_1 u_1^2 + C_2 u_2^2 + C_3 u_3^2 + C_4 u_4^2)]dt.
\end{aligned}
\tag{38}
$$

subject to (36). We associate the coefficients $A_1, A_2, A_3, A_4, C_1, C_2, C_3$ and C_4 to (38) integrand as the weight constants that ensure that Eq. (38) is balanced. The task of the coefficients $A_1, A_2, A_3, A_4, C_1, C_2, C_3$ and C_4 in (38) is that they determine the cost associated with carrying out intervention programmes over a time frame of $[0, T]$. With the state (36), We are looking for the best control $u_1^*, u_2^*, u_3^*, u_4^*$ such that

$$\mathcal{J}(u_1^*, u_2^*, u_3^*, u_4^*) = \min_{\mathcal{U}} \mathcal{J}(u_1, u_2, u_3, u_4). \tag{39}$$

Existence of (u_1, u_2, u_3, u_4)

The results associated with the work of Fleming and Rishel (2012), as has been applied in the works of Nana-Kyere et al. (2022); Asamoah et al. (2017); Okyere et al. (2020) would be employed to show the existence of the optimal control triplets (u_1, u_2, u_3, u_4) that minimizes (38) subject to (36).

Theorem 4.1 *Considering $J(u)$ subject to the model system (36) and with the condition $(S \geq 0, E \geq 0, I \geq 0, H \geq 0, F \geq 0, D \geq 0, B \geq 0, R \geq 0)$, the control u^* exists that minimizes the (36).*

The underlying conditions should be satisfied by proving the existence of the control (36).

Theorem 4.2

(G1) *Convex and closed describe the control set.*
(G2) *The boundary of the system's (36) equation optimization is a linear function in the state and control variables.*
(G3) *Convexity exists between the control and the objective functional (38).*
(G4) *The objective functional (38) integrand is constrained by the following amount by the constants $k_1, k_2 \geq 0$ and $k_3 \geq 1$;*

$$k_1 \left(\sum_{i=1}^{4} |u_i|^2 \right)^{\frac{k_4}{2}} - k_3. \tag{40}$$

Proof

(G1) From (36), $U = [0,1]^4$ represents a closed control set. Further, assigning $h, \nu \in U$, so that $h = (h_1, h_2, h_3, h_4)$ and $\nu = (\nu_1, \nu_2, \nu_3, \nu_4)$. Then for every $\varpi \in [0,1]$, we have $\varpi h_i + (1-\varpi)\nu_i \in U$, which affirms the control set's convexity characteristic.
(G2) The system (36) and the associated results are denoted by χ and ϱ so that the expression $|\chi(t, \varrho_1, u) - \chi(t, \varrho_2, u)|$ is obtained;

$$\begin{aligned}
&\left|-(1-u_1)\alpha_1\left(I_1S_1 - I_2S_2\right)\right| \\
&+ \left|-(1-u_1)\alpha_2\left(H_1S_1 - H_2S_2\right)\right| \\
&+ \left|-(1-u_1)\alpha_3\left(F_1S_1 - F_2S_2\right)\right| \\
&+ \left|-(1-u_1)\alpha_4\left(D_1S_1 - D_2S_2\right)\right| \\
&+ \left|-\mu\left(S_1 - S_2\right)\right| + \left|\rho\left(R_1 - R_2\right)\right| + \left|-u_2\left(S_1 - S_2\right)\right| \\
&+ \left|(1-u_1)\alpha_1\left(I_1S_1 - I_2S_2\right)\right| \\
&+ \left|-(1-u_1)\alpha_2\left(H_1S_1 - H_2S_2\right)\right| \\
&+ \left|-(1-u_1)\alpha_3\left(F_1S_1 - F_2S_2\right)\right| \\
&+ \left|-(1-u_1)\alpha_4\left(D_1S_1 - D_2S_2\right)\right| \\
&+ \left|-(\mu+2\sigma)\left(E_1 - E_2\right)\right| \\
&+ \left|-(\mu+\delta_1+\eta+\phi)\left(I_1 - I_2\right)\right| \\
&+ \left|-k_1\left(F_1 - F_2\right)\right| + \left|(B+u_4+k_2)\left(D_1 - D_2\right)\right| \\
&+ \left|(2\mu+2\delta_2+2y+2u_3+b)\left(H_1 - H_2\right)\right| + \\
&+ \left|(\mu+\rho)\left(R_1 - R_2\right)\right| + \left|-u_2\left(S_1 - S_2\right)\right| \\
&+ \left|-k_3(B_1 - B_2)\right|,
\end{aligned} \tag{41}$$

$$\begin{aligned}
\leq &(1-u_1)\left(2\alpha_1 + 2\alpha_2 + 2\alpha_3 + 2\alpha_4 + 2u_2 + \mu\right)\left|S_1 - S_2\right| \\
&+ (2\sigma+\mu)\left|E_1 - E_2\right| \\
&+ \left(2(1-u_1)\alpha_1 + \mu + \delta_1 + \eta + \phi\right)\left|I_1 - I_2\right| \\
&+ \left(2(1-u_1)\alpha_3 + k_1\right)\left|F_1 - F_2\right| \\
&+ \left(2(1-u_1)\alpha_2 + 2\mu + 2\delta_2 + 2y + 2u_3\right)\left|H_1 - H_2\right| \\
&+ \left(\mu+\rho\right)\left|R_1 - R_2\right| \\
&+ \left(2(1-u_1)\alpha_4 + \beta + u_4 + k_2\right)\left|D_1 - D_2\right| \\
&+ \left(k_3\left|B_1 - B_2\right|\right),
\end{aligned} \tag{42}$$

$$\begin{aligned}
\leq &Z_1\left|S_1 - S_2\right| + Z_2\left|E_1 - E_2\right| + Z_3\left|I_1 - I_2\right| \\
&+ Z_4\left|H_1 - H_2\right| + Z_5\left|F_1 - F_2\right| + Z_6\left|D_1 - D_2\right| \\
&+ Z_7\left|B_1 - B_2\right| + Z_8\left|R_1 - R_2\right|,
\end{aligned} \tag{43}$$

where, $Z_1 = (1-u_1)(2\alpha_1 + 2\alpha_2 + 2\alpha_3 + 2\alpha_4 + 2u_2 + \mu)$,
$Z_2 = (2\sigma + \mu)$,
$Z_3 = \left(2(1-u_1)\alpha_1 + \mu + \delta_1 + \eta + \phi\right)$,
$Z_4 = \left(2(1-u_1)\alpha_2 + 2\mu + 2\delta_2 + 2y + 2u_3\right)$,
$Z_5 = \left(2(1-u_1)\alpha_3 + k_1\right)$,

$Z_6 = \left(2(1-u_1)\alpha_4 + \beta + u_4 + k_2\right)$, $Z_7 = k_3$, $Z_8 = \left(\mu + \rho\right)$ and $Z = \max\{Z_1, Z_2, Z_3, Z_4, Z_5, Z_6, Z_7, Z_8\}$. Hence, it is demonstrated that *chi* has a Lipschitz continuous uniformity.

□

Characterization of optimal control

The Pontryagin's Maximum Principle, an analytical technique that is frequently employed in optimal control, would be used to turn the Ebola model (36) and the objective functional (38) into a problem of minimizing the Hamiltonian H to the controls u_1, u_2, u_3, u_4. The equation's underlying Hamiltonian, Model System (36),

$$H = L(t, \Theta, u) + \sum_{j=1}^{8} \lambda_j f_j. \tag{44}$$

The adjoint variables for the state S, E, I, F, H, D, B, and R are represented by f_j of (44), which is on the right side of (36)

Theorem 4.3 *If the optimum control* (u_1, u_2, u_3, u_4) *meets the requirement* (39),*then there are adjoint variables* ξ_j *that do so below*;

$$\begin{aligned}
\frac{d\lambda_1}{dt} &= \lambda_1\left(\mu + u_2 - \left(u_1 - 1\right)\left(\mathrm{I}\,\alpha_1 + H\,\alpha_2 + F\,\alpha_3 + \mathrm{D}\,\alpha_4\right)\right) \\
&\quad - \lambda_8\, u_2 + \lambda_2\left(u_1 - 1\right)\left(\mathrm{I}\,\alpha_1 + H\,\alpha_2 + F\,\alpha_3 + \mathrm{D}\,\alpha_4\right), \\
\frac{d\lambda_2}{dt} &= \lambda_2\left(\sigma + \mu\right) - A_0 - \lambda_3\,\sigma, \\
\frac{d\lambda_3}{dt} &= \lambda_3\left(\delta_1 + \eta + \mu\right) - \delta_1\,\lambda_6 - \eta\,\lambda_4 \\
&\quad - \lambda_5\,\phi - A_1 - S\,\alpha_1\,\lambda_1\left(u_1 - 1\right) + S\,\alpha_1\,\lambda_2\left(u_1 - 1\right), \\
\frac{d\lambda_4}{dt} &= \lambda_4\left(y + u_3 + \delta_2 + \mu\right) - b\,\lambda_5 \\
&\quad - \delta_2\,\lambda_7 - 2\,\lambda_8\,u_3 - \lambda_6\,y - A_2 - S\,\alpha_2\,\lambda_1\left(u_1 - 1\right) + S\,\alpha_2\,\lambda_2\left(u_1 - 1\right), \\
\frac{d\lambda_5}{dt} &= \kappa_1\,\lambda_5 - A_3 - S\,\alpha_3\,\lambda_1\left(u_1 - 1\right) + S\,\alpha_3\,\lambda_2\left(u_1 - 1\right), \\
\frac{d\lambda_6}{dt} &= \lambda_6\left(u_4 + \kappa_2\right) - A_4 - \beta\,\lambda_5 - \lambda_7\,u_4 \\
&\quad - S\,\alpha_4\,\lambda_1\left(u_1 - 1\right) + S\,\alpha_4\,\lambda_2\left(u_1 - 1\right), \\
\frac{d\lambda_7}{dt} &= \kappa_3\,\lambda_7, \\
\frac{d\lambda_8}{dt} &= \lambda_8\left(\mu + \rho\right) - \lambda_1\,\rho,
\end{aligned} \tag{45}$$

with requirements for transversality

$$\xi_j(T) = 0, \quad j = 1, 2, \ldots, 8. \tag{46}$$

The optimality criterion is satisfied by the control functions $(u_1^*,\ u_2^*,\ u_3^*,\ u_4^*)$, which are provided by

$$u_i^*(t) = \min\left\{1, \max\left\{0, \vartheta_i^*\right\}\right\},\ i = 1,\ 2,\ 3,\ 4, \tag{47}$$

where

$$\begin{aligned}
\vartheta_1^* &= -\frac{\left(\mathrm{I}\,\alpha_1 + H\,\alpha_2 + F\,\alpha_3 + \mathrm{D}\,\alpha_4\right) S\,\lambda_1 + \left(-\mathrm{I}\,\alpha_1 - H\,\alpha_2 - F\,\alpha_3 - \mathrm{D}\,\alpha_4\right) S\,\lambda_2}{C_1}, \\
\vartheta_2^* &= \frac{S\,\lambda_1 - S\,\lambda_8}{C_2}, \quad \vartheta_3^* = \frac{H\,\lambda_4 - H\,\lambda_8}{C_3}, \\
\vartheta_4^* &= \frac{\mathrm{D}\,\lambda_6 - \mathrm{D}\,\lambda_7}{C_4}.
\end{aligned} \tag{48}$$

Proof The Hamiltonian (44) given by;

$$
\begin{aligned}
H = {} & \lambda_4\left(\mathrm{I}\,\eta - H\left(y + u_3 + \delta_2 + \mu\right)\right) - \lambda_2\left(\mathrm{E}\left(\sigma + \mu\right) + S\left(u_1 - 1\right)\left(\mathrm{I}\,\alpha_1 + H\,\alpha_2 + F\,\alpha_3 + \mathrm{D}\,\alpha_4\right)\right) \\
& + \lambda_6\left(\mathrm{I}\,\delta_1 + H\,y - \mathrm{D}\left(u_4 + \kappa_2\right)\right) + \lambda_7\left(\mathrm{D}\,u_4 + H\,\delta_2 - B\,\kappa_3\right) \\
& + \lambda_8\left(2\,H\,u_3 + S\,u_2 - R\left(\mu + \rho\right)\right) + \lambda_5\left(H\,b + \mathrm{D}\,\beta - F\,\kappa_1 + \mathrm{I}\,\phi\right) \\
& + \frac{C_1\,{u_1}^2}{2} + \frac{C_2\,{u_2}^2}{2} + \frac{C_3\,{u_3}^2}{2} + \frac{C_4\,{u_4}^2}{2} + \lambda_3\left(\mathrm{E}\,\sigma - \mathrm{I}\left(\delta_1 + \eta + \mu\right)\right), \\
& + A_4\,\mathrm{D} + A_0\,\mathrm{E} + A_3\,F + A_2\,H + A_1\,\mathrm{I} + \lambda_1\left(\Omega - S\,\mu + R\,\rho - S\,u_2 + S\left(u_1 - 1\right)\left(\mathrm{I}\,\alpha_1 + H\,\alpha_2 + F\,\alpha_3 + \mathrm{D}\,\alpha_4\right)\right),
\end{aligned} \tag{49}
$$

is used to find the adjoint (45) by partial derivative of the Hamiltonian (44) with regards to the model state $S, E, I, H, F, D, B,$ and R as;

$$
\begin{aligned}
&\frac{d\lambda_1}{dt} = -\frac{\partial L}{\partial S}, \frac{d\lambda_2}{dt} = -\frac{\partial L}{\partial E}, \frac{d\lambda_3}{dt} = -\frac{\partial L}{\partial I}, \\
&\frac{d\lambda_4}{dt} = -\frac{\partial L}{\partial H}, \frac{d\lambda_5}{dt} = -\frac{\partial L}{\partial F}, \frac{d\lambda_6}{dt} = -\frac{\partial L}{\partial F}, \\
&\frac{d\lambda_7}{dt} = -\frac{\partial L}{\partial B}, \frac{d\lambda_8}{dt} = -\frac{\partial L}{\partial R}.
\end{aligned} \tag{50}
$$

By using the following equation, the controls $u_1^*, u_2^*, u_3^*, u_4^*$ in (39) are characterized as in (39) as follows:

$$
\frac{\partial L}{\partial u_i} = 0,\ i = 1,\ 2,\ 3,\ 4. \tag{51}
$$

We generate the characterization and apply boundaries to the controls using the standard argument.

$$
u_i^* = \begin{cases} 0 & \text{if } \vartheta_i^* \le 0, \\ \vartheta_1^* & \text{if } 0 \le \vartheta^* \le 1, \\ 1 & \text{if } \vartheta_i^* \ge 1, \end{cases} \tag{52}
$$

where,

$$
\begin{aligned}
&\vartheta_1^* = -\frac{\left(\mathrm{I}\,\alpha_1 + H\,\alpha_2 + F\,\alpha_3 + \mathrm{D}\,\alpha_4\right) S\,\lambda_1 + \left(-\mathrm{I}\,\alpha_1 - H\,\alpha_2 - F\,\alpha_3 - \mathrm{D}\,\alpha_4\right) S\,\lambda_2}{C_1}, \\
&\vartheta_2^* = \frac{S\,\lambda_1 - S\,\lambda_8}{C_2}, \quad \vartheta_3^* = \frac{H\,\lambda_4 - H\,\lambda_8}{C_3}, \\
&\vartheta_4^* = \frac{\mathrm{D}\,\lambda_6 - \mathrm{D}\,\lambda_7}{C_4}.
\end{aligned} \tag{53}
$$

This completes the proof. □

Results

Simulations

Here, numerical examples are provided to complement the analytic method. As Lenhart and Workman (2007) contributed, the forward-backwards sweep is adapted to simulate the control model's optimality system (36). We employed MATLAB software to run the designed model's iterative scheme that used the Runge–Kutta order 4 method to provide the numerical examples. The scheme computed the control state equation forward and the adjoint backwards in time. In a considered interval of [0, 730], the scheme employed initial conditions of the state variables as; 0.7, 0.1, 0.1, 0.1, 0.5, 0.6, 0.1, 0.1 for the classes, S, E, I, H, F, D, B, R respectively, and cost wight unit as: $A_0 = 10, A_1 = 10, A_2 = 10, A_3 = 10, A_4, C_1 = 1, C_2 = 3$, $C_3 = 2$ and $C_4 = 1.5$. Further, the model assumes that $C_2 > C_3 > C_4 > C_1$, since vaccination roll-out programs which constitute the vaccine drug and the implementation of the programme are recognized to be associated with a higher cost than treating the infected and protecting oneself. Hence, we utilized the parameter values in Table 3 for the simulation.

Cost-effectiveness analysis

In this section, cost-effectiveness analysis, which is also known as economic analysis, is utilised to identify the most cost-effective control strategies, as well as the overall most cost-effective intervention of all the control interventions that are currently being investigated and that can be put into place to minimise the objective functional (38) that is subject to the state system (36). The cost-effectiveness analysis can be carried out using either the average cost-effectiveness ratio (ACER) or the incremental cost-effectiveness ratio (ICER), as indicated in the papers (Asamoah et al. 2021; Seidu et al. 2022; Asamoah et al. 2023). Both of these methods are considered to be viable alternatives. A concise

discussion of the two different approaches to cost analysis is presented in the line that immediately follows.

Average cost-effectiveness ratio (ACER)

Average cost-effectiveness ratio is defined as the ratio of the cost related to implementing a particular intervention to the benefit derived from the implementation of the control intervention. In mathematical form, ACER is expressed as

$$ACER = \frac{\text{The complete cost associated with a certain policy}}{\text{Total number of infection cases that the policy prevented}}. \quad (54)$$

As a result, a control intervention plan that has the lowest ACER value is seen as the intervention that offers the most value for the money.

Incremental cost-effectiveness ratio (ICER)

The incremental cost-effectiveness ratio is a valuable tool for determining the difference between the costs of any control intervention techniques vying for the same resource allocation. Consider the possibility that z_1 and z_2 are competing control intervention procedures with the same interest. The ICER may then be calculated by making use of the formula that is presented as

$$ICER = \frac{\text{Cost differences between control strategies } z_1 \text{ and } z_2}{\text{Difference in infection prevented as a result of the strategies}}. \quad (55)$$

The current part takes into account the research of Yang et al. (2018) to determine the most cost-effective method out of those that have been identified for the Ebola model system (36). In Table 4, the number of Ebola virus averted are displayed in ascending order with the accompanying cost involved in each strategy and each ACER.

The calculations from Table 4 reveal that among the offered strategies, strategy 12 has the lowest ACER value. As a result, a control intervention plan that has the lowest ACER value is seen as the intervention that offers the most value for money. Hence, ensuring safe burial and vaccination is regarded as the strategy that is economical in the prevention of Ebola using the proposed model 36. Nonetheless, further investigation of the least cost-effective is necessary in the presence of limited resources. Thus, we calculate the ICER by comparing strategies to each other, and eliminating the one with highest ICER. Therefore, to do this, we regroup Table 4 into single control strategy, double strategy, triple strategy and quadruple strategy with corresponding ICER.

The simulated outcomes of the optimality system, utilising the most effective single control interventions as determined by the ICER calculation in Table 7. The impact of implementing a single vaccine control method (strategy 1, $u_2(t)$) to minimise the objective functional (38) is depicted in Fig. 5. Throughout the intervention period, a decrease in the sizes of exposed individuals (E), symptomatic individuals (I), hospitalised individuals (H), pathogens in the environment (F), and deceased individuals has been noted. The achievement of this objective is realised by consistently keeping the ideal level of vaccination control at a value of 0.75 during the whole duration of the simulation. This suggests that a minimum vaccination rate of 75% is necessary in order to see the reductions in each compartment depicted in Fig. 5a–e, when policymakers choose vaccination as the sole strategy.

Table 4 Optimal control strategies with various ACER

Strategies	Total infection (E,I,H,F,D) Averted	Total cost,$	ACER
Strategy 1	1.7688×10^5	2.0531×10^3	0.0116
Strategy 2	8.9358×10^5	6.1578×10^3	0.0069
Strategy 3	5.5972×10^4	4.0999×10^3	0.0732
Strategy 4	1.9332×10^6	3.0795×10^3	0.0016
Strategy 5	1.7109×10^6	8.2107×10^3	0.0048
Strategy 6	2.3375×10^5	6.1528×10^3	0.0263
Strategy 7	2.2744×10^6	5.1130×10^3	0.0022
Strategy 8	9.5323×10^5	1.0256×10^4	0.0108
Strategy 9	2.2867×10^6	2.3457×10^3	0.0010
Strategy 10	1.9667×10^6	7.1755×10^3	0.0036
Strategy 11	1.7631×10^6	1.2304×10^4	0.0070
Strategy 12	2.2870×10^6	2.2719×10^3	0.00099
Strategy 13	2.2803×10^6	8.2112×10^3	0.0036
Strategy 14	2.2868×10^6	2.7653×10^3	0.0012
Strategy 15	2.2871×10^6	2.7032×10^3	0.0012

The simulated outcomes of the optimality system, utilising the most effective double control interventions as determined by the ICER calculation in Table 12, The impact of implementing vaccination and ensuring a secure burial control method (strategy 9, $u_2(t), u_4(t)$) to minimise the objective functional (38) is depicted in Fig. 6. Throughout the intervention period, the prevalence of Ebola in the exposed compartment (E), symptomatic compartment (I), hospitalised compartment (H), pathogens in the environment (F), and deceased compartment diminished in the course of using vaccination and ensuring a secure burial only. The achievement of this objective is realised by consistently keeping the level of vaccination control at a value of 0.75 for approximately 54 days and ensuring a secure burial control at a value of 0.75 for approximately 90 days, then gradually decreasing the vaccination control to 0.25 at approximately day 252 and keeping constant during the whole duration of the simulation, and also gradually decreasing the ensuring a secure burial control to 0.25 at approximately day 280 and

keeping constant during the whole duration of the simulation. This suggests that a minimum vaccination rate of 75% for 54 days and 75% of ensuring a secure burial for 90 days, and a minimum vaccination rate 25% at day 252 and a minimum 25% at day 280 are necessary in order to see the reductions in each compartment depicted in Fig. 6a–e, when policymakers choose vaccination and ensuring a secure burial as the sole control measures.

The simulated outcomes of the optimality system, utilising the most effective triple control interventions as determined by the ICER calculation in Table 15, The impact of implementing personal protection, vaccination and ensuring a secure burial control method (strategy 9, $u_1(t)$, $u_2(t), u_4(t)$) to minimise the objective functional (36) is depicted in Fig. 7. Throughout the intervention period, the prevalence of Ebola in the exposed compartment (E), symptomatic compartment (I), hospitalised compartment (H), pathogens in the environment (F), and deceased compartment diminished in the course of simultaneously using personal protection, vaccination and ensuring a secure burial only. The achievement of this objective is realised by consistently keeping the level of personal protection control at a value of 0.75 for approximately 98 days, vaccination control at a value of 0.75 for approximately 47 days and ensuring a secure burial control at a value of 0.75 for approximately 10 days, then gradually decreasing personal protection to 0.5 at approximately day 21, further to 0.25 at day 186 and finally keeping constant during the whole duration of the simulation. The vaccination control should be reduced to 0.25 at approximately day 228 and keeping constant during the whole duration of the simulation, and also gradually decreasing the ensuring a secure burial control to 0.25 at approximately day 256 and keeping constant during the whole duration of the simulation. This suggests that a minimum 75% of the population should practice personal protection during the peak of Ebola for 10 day, vaccination rate of 75% for 47 days and 75% of ensuring a secure burial for 10 days, and a minimum 25% for personal protection, vaccination, and ensuring a secure burial for the rest of two years in order to see the reductions in each compartment depicted in Fig. 7a–e, when policymakers choose personal protection, vaccination and ensuring a secure burial as the sole control measures.

The impact of implementing personal protection, vaccination treatment and ensuring a secure burial control method (strategy 9, $u_1(t)$, $u_2(t), u_3(t), u_4(t)$) to minimise the objective functional (38) is depicted in Fig. 8. Throughout the intervention period, the prevalence of Ebola in the exposed compartment (E), symptomatic compartment (I), hospitalised compartment (H), pathogens in the environment (F), and deceased compartment diminished in the course of simultaneously using personal protection, vaccination, treatment and ensuring a secure burial. The achievement of this objective is realised by consistently keeping the level of personal protection, vaccination, treatment and ensuring a secure burial control at a value of 0.75 for approximately 95, 40, 2 and 7 days respectively, then gradually decreasing personal protection to 0.25 at approximately day 249, finally keeping constant during the whole duration of the simulation. The vaccination control should be reduced to 0.25 at approximately day 201 and keeping constant during the whole duration of the simulation. The treatment control should be reduced to 0.27 at approximately day 11, and keeping constant during the whole duration of the simulation and also gradually decreasing the ensuring a secure burial control to 0.5 at approximately day 14, then to 0.25 at approximately day 169 and keeping constant during the whole duration of the simulation. This suggests that a minimum 75% of the population should practice personal protection during the peak of Ebola for 95 day, vaccination rate of 75% for 40 days, treatment 75% for 2 days and 75% of ensuring a secure burial for 7 days, and a minimum 25% for personal protection, vaccination, treatment and ensuring a secure burial for the rest of two years in order to see the reductions in each compartment depicted in Fig. 8a–e, when policymakers choose personal protection, vaccination, treatment and ensuring a secure burial as control measures.

Discussion

ICER for single control strategies

The incremental cost-effectiveness ratios (ICERs) for the four individual intervention options in the single control group are explicitly calculated using the methodology shown in (55). The computational findings are shown in Table 5. Upon examination of the single intervention strategies 1 and 4 as presented in Table 5, it is evident that the ICER value associated with intervention strategy 4 is lower than the ICER value associated with intervention strategy 1. The economic implication of this finding is that strategy 4 exhibits a much superior performance compared to strategy 1. Therefore, it can be concluded that single intervention strategy 4 exhibits superior effectiveness at a more affordable cost compared to single intervention 1. Currently, intervention strategy 1 has been excluded from the pool of interventions vying for the same allocation, however intervention strategy 4 remains included. The ICER value for intervention approach 4 remains unchanged, as seen in Table 4. However, the ICER for the individual intervention 4 is recalculated using the formula (55). Upon comparing the ICER values of strategy 4 and strategy 3, it becomes apparent that strategy 4 exhibits a greater ICER in comparison to strategy 3. This shows that strategy 3 considerably dominates strategy 4. Thus, in comparison to strategy 3, strategy 4 exhibits higher costs and worse efficacy in its implementation (Table 6). Given the circumstances, intervention approach 4 has been

Table 5 Single control, infections prevented beginning with the smallest to the greatest

Strategies	Total infection (E,I,H,F,D) Averted	Total cost,$	ICER
Strategy 1	1.7688×10^5	2.0531×10^3	0.0116
Strategy 4	1.9332×10^6	3.0795×10^3	5.8440×10^{-4}
Strategy 3	5.5972×10^4	4.0999×10^3	-5.4357×10^{-4}
Strategy 2	8.9358×10^5	6.1578×10^3	0.0025

Table 6 Single control, infections prevented beginning with the smallest to the greatest

Strategies	Total infection (E,I,H,F,D) Averted	Total cost,$	ICER
Strategy 4	1.9332×10^6	3.0795×10^3	0.0016
Strategy 3	5.5972×10^4	4.0999×10^3	-5.4357×10^{-4}
Strategy 2	8.9358×10^5	6.1578×10^3	0.0025

Table 7 Single control, infections prevented beginning with the smallest to the greatest

Strategies	Total infection (E,I,H,F,D) Averted	Total cost,$	ICER
Strategy 3	5.5972×10^4	4.0999×10^3	0.0732
Strategy 2	8.9358×10^5	6.1578×10^3	0.0025

excluded from the pool of strategies vying for the same resources. Hence, the ICER for the individual intervention 3 is recalculated using the formula (55), as shown in Table 7. Upon comparing the ICER values of strategy 3 and strategy 2, it becomes apparent that strategy 3 exhibits a greater ICER in comparison to strategy 2. This shows that strategy 2 considerably dominates strategy 3. Thus, in comparison to strategy 2, strategy 3 exhibits higher costs and worse efficacy in its implementation. Therefore, the utilisation of the ICER approach reveals that among the many single control techniques, the intervention labelled as "vaccination" (referred to as intervention 2) proves to be the most cost-effective. The observed result aligns with the cost analysis methodology employed by ACER. Figure 5, shows the simulation trajectories of the exposed, symptomatic, hospitalized, pathogenes in the environment, deceased compartments and the optimal control profile of strategy 2. All other Figures associated with the other single control strategies are ignored.

ICER for double control strategies

The incremental cost-effectiveness ratios (ICERs) for the six grouped intervention options in the double control strategies are explicitly calculated using the methodology shown in (55). The computational findings are shown in Table 8. Upon examination of the double intervention strategies 6 and 8 as presented in Table 8, it is evident that the ICER value associated with intervention strategy 8 is lower than the ICER value associated with intervention strategy 6. The economic implication of this finding is that strategy 8 exhibits a much superior performance compared to strategy 6. Therefore, it can be concluded that double intervention strategy 8 exhibits superior effectiveness at a more affordable cost compared to single intervention 6. Hence, intervention strategy 6 has been excluded from the pool of interventions vying for the same allocation, however intervention strategy 8 remains included. The ICER for the individual intervention 8 is recalculated using the formula (55). Upon comparing the ICER values of strategy 8 and strategy 5 in Table 9, it becomes apparent that strategy 8 exhibits a greater ICER in comparison to strategy 5. This shows that strategy 5 considerably dominates strategy 8. Thus, in comparison to strategy 5, strategy 8 exhibits higher costs and worse efficacy in its implementation. Given the circumstances, intervention approach 8 has been excluded from the pool of strategies vying for the same resources. Hence, the ICER for the individual intervention 5 is recalculated using the formula (55), as shown in Table 10. Upon comparing the ICER values of strategy 5 and strategy 10, it becomes apparent that strategy 5 exhibits a greater ICER in comparison to strategy 10. This shows that strategy 10 considerably dominates strategy 5. Thus, in comparison to strategy 10, strategy 5 exhibits higher costs and worse efficacy in its implementation. Hence, intervention strategy 5 has been excluded from the pool of interventions vying for the same allocation, however intervention strategy 10 remains included. The ICER for the individual intervention 9 is recalculated using the formula (55) as shown in Table 11. Upon comparing the ICER values of strategy 10 and strategy 7, it becomes apparent that strategy 10 exhibits a greater ICER in comparison to strategy 7. This shows that strategy 7 considerably dominates strategy 10. Thus, in comparison to strategy 7, strategy 10 exhibits higher costs and worse efficacy in its implementation. Hence, intervention strategy 10 has been excluded from the pool of interventions vying for the same allocation, however intervention strategy 7 remains included. The ICER for the double intervention 7 is recalculated using the formula (55) as shown in Table 12. Upon comparing the ICER values of strategy 7 and strategy 9, it becomes apparent that strategy 7 exhibits a greater ICER in comparison to strategy 9. This shows that strategy 9 considerably dominates strategy 7. Thus, in comparison to strategy 9, strategy 7 exhibits higher costs and worse efficacy in its implementation. Therefore, the utilisation of the ICER approach reveals that among the many double control techniques, the intervention labelled as "vaccination and ensuring a secure burial" (referred to as intervention 9) proves to be the most cost-effective. The

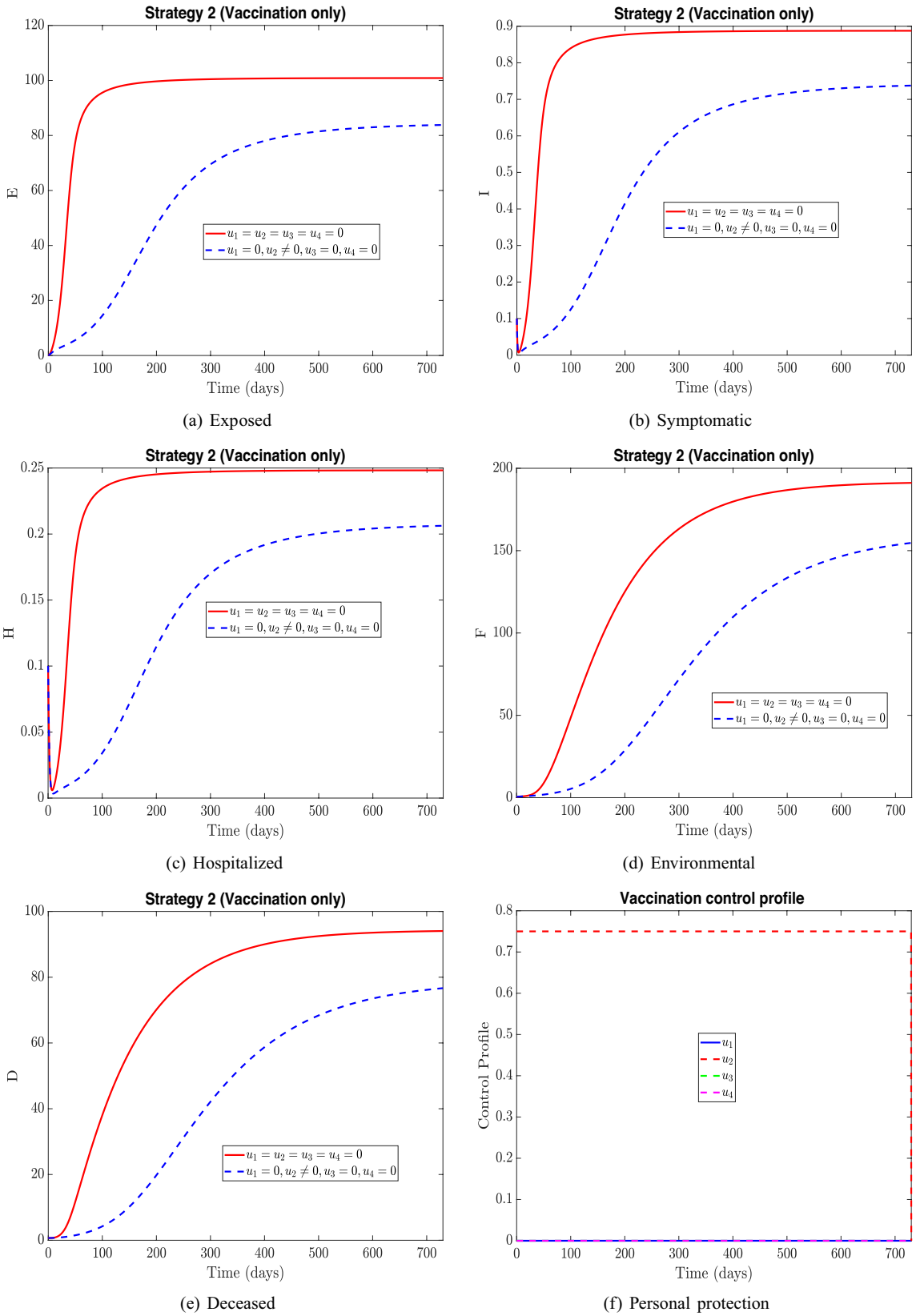

(a) Exposed (b) Symptomatic

(c) Hospitalized (d) Environmental

(e) Deceased (f) Personal protection

Fig. 5 Solution paths of the exposed, symptomatic, hospitalized, environmental, deceased with vaccination only

Table 8 Double control, infections prevented beginning with the smallest to the greatest

Strategies	Total infection (E,I,H,F,D) Averted	Total cost,$	ICER
Strategy 6	2.3375×10^5	6.1528×10^3	0.0263
Strategy 8	9.5323×10^5	1.0256×10^4	0.0057
Strategy 5	1.7109×10^6	8.2107×10^3	– 0.0027
Strategy 10	1.9667×10^6	7.1755×10^3	– 0.0040
Strategy 7	2.2744×10^6	5.1130×10^3	– 0.0067
Strategy 9	2.2867×10^6	2.3457×10^3	– 0.2250

Table 9 Double control, infections prevented beginning with the smallest to the greatest

Strategies	Total infection (E,I,H,F,D) Averted	Total cost,$	ICER
Strategy 8	9.5323×10^5	1.0256×10^4	0.0108
Strategy 5	1.7109×10^6	8.2107×10^3	– 0.0027
Strategy 10	1.9667×10^6	7.1755×10^3	– 0.0040
Strategy 7	2.2744×10^6	5.1130×10^3	– 0.0067
Strategy 9	2.2867×10^6	2.3457×10^3	– 0.2250

Table 10 Double control, infections prevented beginning with the smallest to the greatest

Strategies	Total infection (E,I,H,F,D) Averted	Total cost,$	ICER
Strategy 5	1.7109×10^6	8.2107×10^3	0.0048
Strategy 10	1.9667×10^6	7.1755×10^3	– 0.0040
Strategy 7	2.2744×10^6	5.1130×10^3	– 0.0067
Strategy 9	2.2867×10^6	2.3457×10^3	– 0.2250

Table 11 Double control, infections prevented beginning with the smallest to the greatest

Strategies	Total infection (E,I,H,F,D) Averted	Total cost,$	ICER
Strategy 10	1.9667×10^6	7.1755×10^3	0.0036
Strategy 7	2.2744×10^6	5.1130×10^3	– 0.0067
Strategy 9	2.2867×10^6	2.3457×10^3	– 0.2250

observed result is aligns with the cost analysis methodology employed by ACER. Figure 6, shows the simulation trajectories of the exposed, symptomatic, hospitalized, pathogenes in the environment, deceased compartments and the optimal control profile of strategy 9. All other Figures associated with the other double control strategies are ignored.

Table 12 Double control, infections prevented beginning with the smallest to the greatest

Strategies	Total infection (E,I,H,F,D) Averted	Total cost,$	ICER
Strategy 7	2.2744×10^6	5.1130×10^3	0.0022
Strategy 9	2.2867×10^6	2.3457×10^3	– 0.2250

ICER for triple controls strategies

The incremental cost-effectiveness ratios (ICERs) for the four grouped intervention options in the triple control strategies are explicitly calculated using the methodology shown in equation (55). The computational findings are shown in Table 13. Upon examination of the double intervention strategies 11 and 13 as presented in Table 13, it is evident that the ICER value associated with intervention strategy 13 is lower than the ICER value associated with intervention strategy 11. The economic implication of this finding is that strategy 13 exhibits a much superior performance compared to strategy 11. Therefore, it can be concluded that double intervention strategy 13 exhibits superior effectiveness at a more affordable cost compared to single intervention 11. Hence, intervention strategy 11 has been excluded from the pool of interventions vying for the same allocation, however intervention strategy 13 remains included. The ICER for the intervention 13 is recalculated using the formula (55). Upon comparing the ICER values of strategy 13 and strategy 14 in Table 14, it becomes apparent that strategy 13 exhibits a greater ICER in comparison to strategy 14. This shows that strategy 14 considerably dominates strategy 13. Thus, in comparison to strategy 14, strategy 13 exhibits higher costs and worse efficacy in its implementation. Given the circumstances, intervention approach 13 has been excluded from the pool of strategies vying for the same resources. Hence, the ICER for the intervention 14 is recalculated using the formula (55), as shown in Table 15. Upon comparing the ICER values of strategy 14 and strategy 12, it becomes apparent that strategy 14 exhibits a greater ICER in comparison to strategy 12. Thus, in comparison to strategy 12, strategy 14 exhibits higher costs and worse efficacy in its implementation. Therefore, the utilisation of the ICER approach reveals that among the many triple control techniques, the intervention labelled as "personal protection, vaccination and ensuring a secure burial" (referred to as intervention 12) proves to be the most cost-effective. The observed result is aligns with the cost analysis methodology employed by ACER. Figure 7, shows the simulation trajectories of the exposed, symptomatic, hospitalized, pathogenes in the environment, deceased compartments and the optimal control profile of strategy 12. All other Figures associated with the other double control strategies are ignored.

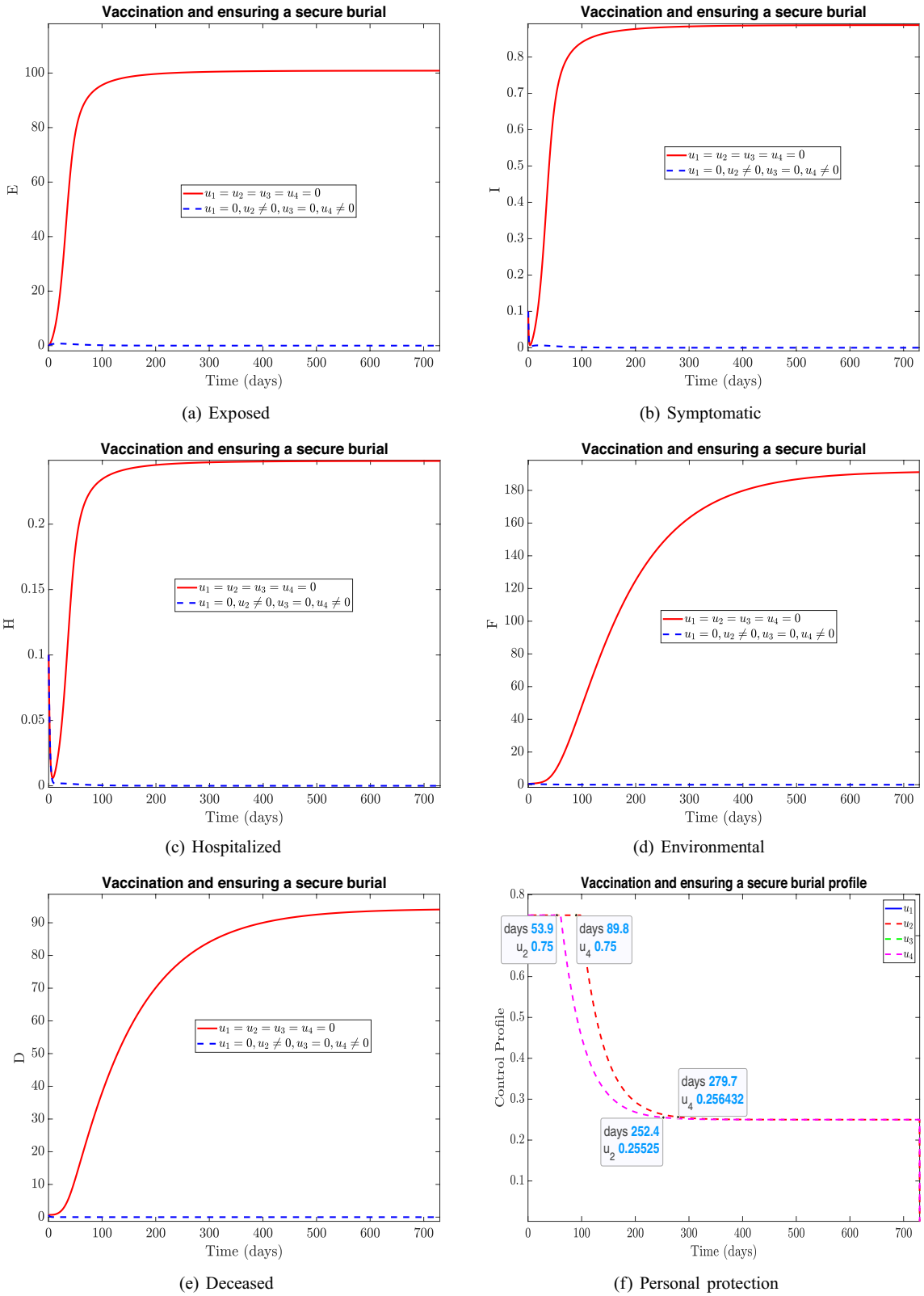

(a) Exposed (b) Symptomatic

(c) Hospitalized (d) Environmental

(e) Deceased (f) Personal protection

Fig. 6 Solution paths of the exposed, symptomatic, hospitalized, environmental, deceased with vaccination and ensuring a secure burial only

Table 13 Triple controls, infections prevented beginning with the smallest to the greatest

Strategies	Total infection (E,I,H,F,D) Averted	Total cost,$	ICER
Strategy 11	1.7631×10^6	1.2304×10^4	0.0070
Strategy 13	2.2803×10^6	8.2112×10^3	– 0.0079
Strategy 14	2.2868×10^6	2.7653×10^3	– 0.8378
Strategy 12	2.2870×10^6	2.2719×10^3	– 2.4670

Table 14 Triple controls, infections prevented beginning with the smallest to the greatest

Strategies	Total infection (E,I,H,F,D) Averted	Total cost,$	ICER
Strategy 13	2.2803×10^6	8.2112×10^3	0.0036
Strategy 14	2.2868×10^6	2.7653×10^3	– 0.8378
Strategy 12	2.2870×10^6	2.2719×10^3	– 2.4670

Table 15 Triple controls, infections prevented beginning with the smallest to the greatest

Strategies	Total infection (E,I,H,F,D) Averted	Total cost,$	ICER
Strategy 14	2.2868×10^6	2.7653×10^3	0.0012
Strategy 12	2.2870×10^6	2.2719×10^3	– 2.4670

ICER implementation of quadruple control

In this case, there is no requirement for comparison because implementation of quadruple control only uses one group of intervention strategy, which is the combination of the four control variables (u_1, u_2, u_3, u_4). Therefore, this intervention strategy has the same ICER value with ACER value as given in Table 4. Figure 8, shows the simulation trajectories of the exposed, symptomatic, hospitalized, pathogenes in the environment, deceased compartments and the optimal control profile of strategy 15 (implementation of quadruple control).

ICER of the most cost-effective interventions among the best controls

Here, out of all the potential control combination strategies, the ICER method is used to confirm the most cost-effective intervention in the long run. Based on the conclusions of the ICER approach, the following intervention options were chosen: strategy 2, 9, 12, and strategy 15 as shown in Table 16. The ICER value for the single intervention strategy 2 is higher than the ICER value for the double intervention strategy 9 when comparing control and intervention strategies 2 and 9. Because of its higher cost and worse effectiveness, strategy 2 is eliminated from consideration in favour of strategy 9. Table 17 shows the results of the ICER recalculations for strategies 9. The ICER value for the double intervention strategy 9 is higher than the ICER value for the triple intervention strategy 12 when comparing control and intervention strategies 9 and 12. Because of its higher cost and worse effectiveness, strategy 9 is eliminated from consideration in favour of strategy 12. Table 18 shows the results of the ICER recalculations for strategies 12. The ICER value for the quadruple intervention strategy 15 is higher than the ICER value for the triple intervention strategy 12 when comparing control and intervention strategies 12 and 15. Because of its higher cost and worse effectiveness, strategy 12 is the most effective strategy and economical among all the control strategies.

Conclusion

We examined a SEIHRFDBR transmission model of Ebola dynamics capturing the disease transmission with environmental contamination of the virus. We estimated the basic reproduction number and discussed the existence of Ebola-free and Ebola-present equilibria. Furthermore, we found the conditions where bifurcation might occur by applying bifurcation theory to Ebola model (2). The diagram of the forward bifurcation phenomenon is shown in Fig. 2. With the initial conditions and model input, we examined the parameters that caused variability in the $\mathcal{R}_0$ by carrying out a sensitivity analysis of the reproduction number. The sensitivity analysis assists to design the formulation of the optimal control model by deducing strategies that would help lower the transmissible probability per contact of the infected and susceptible individuals. The analysis, therefore, indicates that contact between susceptible and dead Ebola individuals, contaminated Ebola environment due to the shedding of the virus by (dead and alive) infected individuals, and direct contact with infected individuals has to be minimized through sensitization of the communities to manage the disease. Further, we encourage stakeholder engagement with the communities to ensure that infectious Ebola victims are transferred to the various health facilities for treatment, as the analysis indicated that increasing hospitalization for treatment reduces $\mathcal{R}_0$. Finally, the analysis proved that practising safe burial for infected Ebola victims decreases the $\mathcal{R}_0$. Hence, we recommend that concerned decision-making bodies should ensure that dead Ebola victims are transferred from the hospitals to appropriate authorities for safer burials. We now create an optimal control model from the state model (2) based on the findings of the sensitivity analysis, adding time-dependent controls for personal protection, vaccination, and treatment to model (2) to identify a range of workable methods for eradicating the disease.

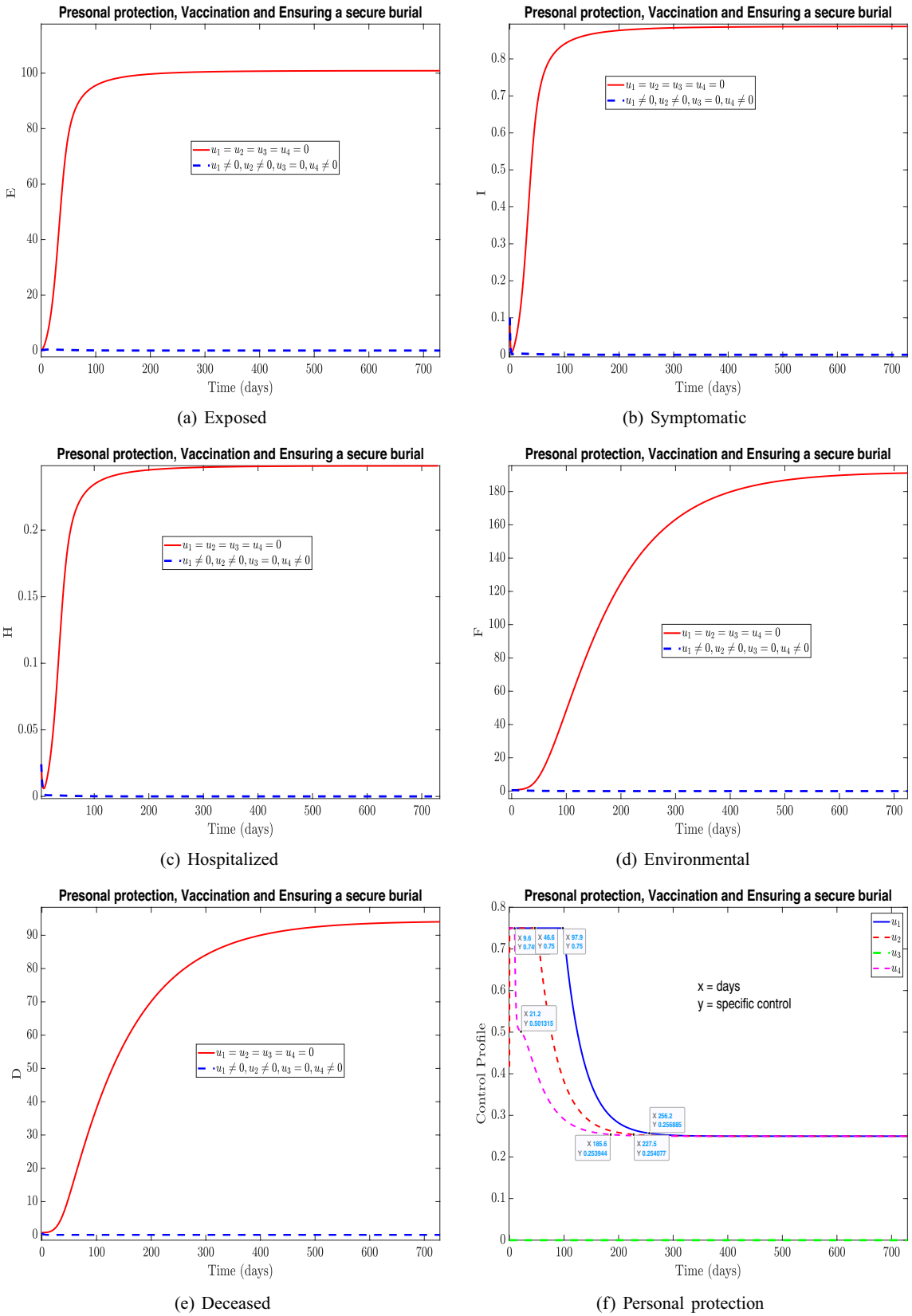

Fig. 7 Solution paths of the exposed, symptomatic, hospitalized, environmental, deceased with personal protection, vaccination and ensuring a secure burial only

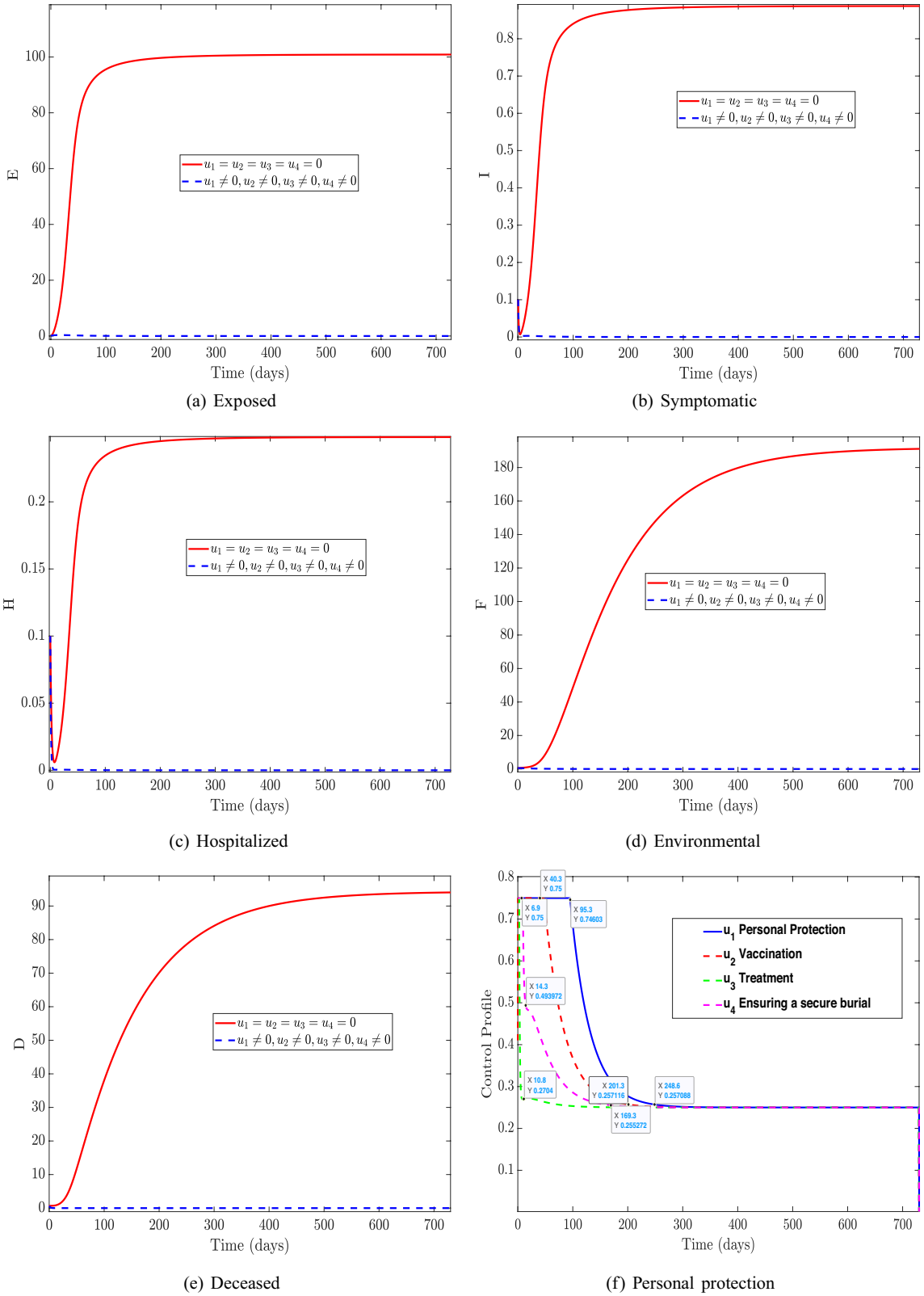

(a) Exposed (b) Symptomatic

(c) Hospitalized (d) Environmental

(e) Deceased (f) Personal protection

Fig. 8 Solution paths of the exposed, symptomatic, hospitalized, environmental, deceased with personal protection, vaccination, treatment and ensuring a secure burial

Table 16 most cost-effective interventions among the best controls

Strategies	Total infection (E,I,H,F,D) Averted	Total cost,$	ICER
Strategy 2	8.9358×10^5	6.1578×10^3	0.0069
Strategy 9	2.2867×10^6	2.3457×10^3	– 0.0027
Strategy 12	2.2870×10^6	2.2719×10^3	– 0.2460
Strategy 15	2.2871×10^6	2.7032×10^3	4.3130

Table 17 most cost-effective interventions among the best controls

Strategies	Total infection (E,I,H,F,D) Averted	Total cost,$	ICER
Strategy 9	2.2867×10^6	2.3457×10^3	0.0010
Strategy 12	2.2870×10^6	2.2719×10^3	– 0.2460
Strategy 15	2.2871×10^6	2.7032×10^3	4.3130

Table 18 most cost-effective interventions among the best controls

Strategies	Total infection (E,I,H,F,D) Averted	Total cost,$	ICER
Strategy 12	2.2870×10^6	2.2719×10^3	0.00099
Strategy 15	2.2871×10^6	2.7032×10^3	4.3130

By transforming the objective functional and the state (2) into a minimization problem, the control model is solved analytically using Pontryagin's maximal principle. With the aid of MATLAB, an iterative scheme is designed that uses a fourth-order Runge–Kutta to numerically solves the control model. The scheme employs a set of codes that solves the state equation forward in time and the adjoint system backwards in time. The scheme runs until a specified stopping criterion is reached. Lastly, to determine the cost involved with the implementation of the strategies, an in-depth cost analysis was undertaken to find out the strategy that brings the best output of minimizing the Ebola disease but has the least cost. The analysis revealed that strategy 12 (personal protection, vaccination and ensuring a secure burial) is the most cost-effective strategy within the considered strategies.

Acknowledgements The authors are thankful to the handling editor and anonymous reviewers for their constructive comments and suggestions that led to the presentation of this improved manuscript.

Author Contributions The authors confirm sole responsibility for study conceptualization, methodology, formal analysis, codes writing, manuscript writing and editing, and approval of the final manuscript draft. Isaac Kwasi Adu: conceptualization, methodology, formal analysis, writing, review, and editing. Fredrick Asenso Wireko: methodology, formal analysis, writing, review, and editing. Sacrifice Nana-Kyere: conceptualization, methodology, formal analysis. Ebenezer Appiagyei: original draft, writing. Mojeeb AL-Rahman EL-Nor Osman: original draft, writing. Joshua Kiddy K. Asamoah: methodology, supervision, formal analysis, writing, review, and editing.

Funding No funds, grants, or other support were received.

Availability of data and materials The authors confirm that the data supporting the findings of this study are available within the article.

Code availability Matlab code is available from the author on reasonable request.

Declarations

Conflict of interest The authors has no Conflict of interest to declare that are relevant to the content of this article.

References

Abidemi A (2023) Optimal cost-effective control of drug abuse by students: insight from mathematical modeling. Model Earth Syst Environ 9:811–829

Adu IK, Wireko FA, Sebil C, Asamoah JKK (2023) A fractal-fractional model of Ebola with reinfection. Results Phys 52:106893

Ahmad YU, Andrawus J, Ado A, Maigoro YA, Yusuf A, Althobaiti S, Mustapha UT (2024) Mathematical modeling and analysis of human-to-human Monkeypox virus transmission with post-exposure vaccination. Model Earth Syst Environ 1–21

Ahmad MD, Usman M, Khan A, Imran M (2016) Optimal control analysis of Ebola disease with control strategies of quarantine and vaccination. Infect Dis Poverty 5:1–12

Alade TO, Alnegga M, Olaniyi S, Abidemi A (2023) Mathematical modelling of within-host chikungunya virus dynamics with adaptive immune response. Model Earth Syst Environ 9:3837–3849

Alla Hamou A, Azroul E, Bouda S, Guedda M (2024) Mathematical modeling of HIV transmission in a heterosexual population: incorporating memory conservation. Model Earth Syst Environ 10:393–416

Asamoah J KK, Oduro FT, Bonyah E, Seidu B (2017) Modelling of rabies transmission dynamics using optimal control analysis. J Appl Math **2017**

Asamoah J KK, Safianu B, Afrifa E, Obeng B, Seidu B, Wireko FA, Sun G-Q (2023) Optimal control dynamics of gonorrhea in a structured population. Heliyon **9**

Asamoah JKK, Owusu MA, Jin Z, Oduro F, Abidemi A, Gyasi EO (2020) Global stability and cost-effectiveness analysis of Covid-19 considering the impact of the environment: using data from ghana. Chaos Solit Fractals 140:110103

Asamoah JKK, Jin Z, Sun G-Q (2021) Non-seasonal and seasonal relapse model for q fever disease with comprehensive cost-effectiveness analysis. Results Phys 22:103889

Berge T, Lubuma J-S, Moremedi G, Morris N, Kondera-Shava R (2017) A simple mathematical model for Ebola in Africa. J Biol Dyn 11:42–74

Brauer F, Castillo-Chavez C, Castillo-Chavez C (2012) Mathematical models in population biology and epidemiology, vol 2. Springer

Bray M, Hirsch M, Mitty J (2014) Epidemiology, pathogenesis, and clinical manifestations of Ebola and Marburg virus disease. Update 43:65–9

Buonomo B, Lacitignola D (2010) Analysis of a tuberculosis model with a case study in Uganda. J Biol Dyn 4:571–593

Castillo-Chavez C, Song B (2004) Dynamical models of tuberculosis and their applications. Math Biosci Eng 1:361

Chan M (2014) Ebola virus disease in west Africa-no early end to the outbreak. N Engl J Med 371:1183–1185
Chen J, Huang J, Beier JC, Cantrell RS, Cosner C, Fuller DO, Zhang G, Ruan S (2016) Modeling and control of local outbreaks of west Nile virus in the United States. Discrete Continu Dyn Syst-B 21:2423
Chitnis N, Hyman JM, Cushing JM (2008) Determining important parameters in the spread of malaria through the sensitivity analysis of a mathematical model. Bull Math Biol 70:1272–1296
Chowell G, Nishiura H (2014) Transmission dynamics and control of Ebola virus disease (evd): a review. BMC Med 12:1–17
Conrad JR, Xue L, Dewar J, Hyman JM (2016) Modeling the impact of behavior change on the spread of Ebola. In Mathematical and statistical modeling for emerging and re-emerging infectious diseases (pp 5–23). Springer
Das DK, Khajanchi S, Kar T (2020) Transmission dynamics of tuberculosis with multiple re-infections. Chaos Solit Fractals 130:109450
Das DK, Khajanchi S, Kar TK (2020) The impact of the media awareness and optimal strategy on the prevalence of tuberculosis. Appl Math Comput 366:124732
Dowell SF, Mukunu R, Ksiazek TG, Khan AS, Rollin PE, Peters CJ (1999) Transmission of Ebola hemorrhagic fever: a study of risk factors in family members, kikwit, democratic republic of the congo, 1995. J Infect Dis 179:S87–S91
Edith DN, Mbah GCE, Bassey BE (2020) Optimal control analysis model of Ebola virus infection: impact of socio-economic status. Int J Appl Sci Math 6:2394–2894
Edward S, Lusekelo EM, Ndidi DM, Simanjilo E (2017) Mathematical modelling of the transmission dynamics of Ebola virus disease with control strategies. Int J Sci 33:112–130
Feldmann H, Geisbert TW (2011) Ebola haemorrhagic fever. The Lancet 377:849–862
Fisman D, Khoo E, Tuite A (2014) Early epidemic dynamics of the west African 2014 Ebola outbreak: estimates derived with a simple two-parameter model. PLoS Curr 6
Fleming WH, Rishel RW (2012) Deterministic and stochastic optimal control volume 1. Springer Science & Business Media
Gomes MF, y Piontti AP, Rossi L, Chao D, Longini I, Halloran ME, Vespignani A (2014) Assessing the international spreading risk associated with the 2014 west African Ebola outbreak. PLoS Curr 6
Heffernan RT, Pambo B, Hatchett RJ, Leman PA, Swanepoel R, Ryder RW (2005) Low seroprevalence of igg antibodies to Ebola virus in an epidemic zone: Ogooue-Ivindo region, northeastern Gabon, 1997. J Infect Dis 191:964–968
Imran M, Khan A, Ansari AR, Shah STH (2017) Modeling transmission dynamics of Ebola virus disease. Int J Biomath 10:1750057
Jones SM, Feldmann H, Ströher U, Geisbert JB, Fernando L, Grolla A, Klenk H-D, Sullivan NJ, Volchkov VE, Fritz EA et al (2005) Live attenuated recombinant vaccine protects nonhuman primates against Ebola and Marburg viruses. Nat Med 11:786–790
Juga M, Nyabadza F, Chirove F (2021) An Ebola virus disease model with fear and environmental transmission dynamics. Infect Dis Modell 6:545
Khajanchi S, Ghosh D (2015) The combined effects of optimal control in cancer remission. Appl Math Comput 271:375–388
Khajanchi S, Das DK, Kar TK (2018) Dynamics of tuberculosis transmission with exogenous reinfections and endogenous reactivation. Physica A 497:52–71
Khajanchi S, Sarkar K, Mondal J, Nisar KS, Abdelwahab SF (2021) Mathematical modeling of the Covid-19 pandemic with intervention strategies. Results Phys 25:104285
Lamunu M, Lutwama J, Kamugisha J, Opio A, Nambooze J, Ndayimirije N, Okware S (2004) Containing a haemorrhagic fever epidemic: the Ebola experience in Uganda (October 2000–January 2001). Int J Infect Dis 8:27–37
Lashari AA, Zaman G (2012) Optimal control of a vector borne disease with horizontal transmission. Nonlinear Anal Real World Appl 13:203–212
Legrand J, Grais RF, Boelle P-Y, Valleron A-J, Flahault A (2007) Understanding the dynamics of Ebola epidemics. Epidemiol Infect 135:610–621
Lenhart S, Workman JT (2007) Optimal control applied to biological models. Chapman and Hall/CRC
Leroy EM, Baize S, Volchkov V, Fisher-Hoch S, Georges-Courbot M, Lansoud-Soukate J, Capron M, Debre P, Georges A, McCormick J (2000) Human asymptomatic Ebola infection and strong inflammatory response. The Lancet 355:2210–2215
Mabotsa M, Munganga JMW, Hassan AS (2022) Mathematical modelling and optimal control of the transmission dynamics of enterovirus. Phys Scr 97:034002
MacIntyre CR, Chughtai AA (2016) Recurrence and reinfection-a new paradigm for the management of Ebola virus disease. Int J Infect Dis 43:58–61
Mhlanga A (2019) Dynamical analysis and control strategies in modelling Ebola virus disease. Adv Difference Equ 2019:1–27
Mondal J, Khajanchi S, Samui P (2022) Impact of media awareness in mitigating the spread of an infectious disease with application to optimal control. Eur Phys J Plus 137:983
Mugabi F, Duffy KJ, van Langevelde F (2024) Behaviours of honeybees can reduce the probability of deformed wing virus outbreaks in varroa destructor-infested colonies. Model Earth Syst Environ 1–17
Nana-Kyere S, Boateng FA, Jonathan P, Donkor A, Hoggar GK, Titus BD, Kwarteng D, Adu IK (2022) Global analysis and optimal control model of Covid-19. Comput Math Methods Med. 2022
Ndanguza D, Tchuenche J, Haario H (2013) Statistical data analysis of the 1995 Ebola outbreak in the democratic republic of Congo. Afr Mat 24:55–68
Okyere E, Olaniyi S, Bonyah E (2020) Analysis of zika virus dynamics with sexual transmission route using multiple optimal controls. Sci Afr 9:e00532
Peter OJ, Kumar S, Kumari N, Oguntolu FA, Oshinubi K, Musa R (2022) Transmission dynamics of monkeypox virus: a mathematical modelling approach. Model Earth Syst Environ 1–12
Rachah A, Torres DF (2015) Mathematical modelling, simulation, and optimal control of the 2014 Ebola outbreak in west Africa. Discrete Dyn Nat Soc 2015
Roca A, Afolabi MO, Saidu Y, Kampmann B (2015) Ebola: a holistic approach is required to achieve effective management and control. J Allergy Clin Immunol 135:856–867
Rosenke K, Adjemian J, Munster VJ, Marzi A, Falzarano D, Onyango CO, Ochieng M, Juma B, Fischer RJ, Prescott JB et al (2016) Plasmodium Parasitemia associated with increased survival in Ebola virus-infected patients. Clin Infect Dis 63:1026–1033
Sahu I, Jena SR (2023) Sdiqr mathematical modelling for Covid-19 of Odisha associated with influx of migrants based on laplace adomian decomposition technique. Model Earth Syst Environ 9:4031–4040
Seck R, Ngom D, Ivorra B, Ramos ÁM (2022) An optimal control model to design strategies for reducing the spread of the Ebola virus disease. Math Biosci Eng 19:1746–1774
Seidu B, Asamoah JKK, Wiah EN, Ackora-Prah J (2022) A comprehensive cost-effectiveness analysis of control of maize streak virus disease with Holling's type ii predation form and standard incidence. Results Phys 40:105862
Sharma S, Samanta G (2017) Analysis of a hand-foot-mouth disease model. Int J Biomath 10:1750016
Siettos C, Anastassopoulou C, Russo L, Grigoras C, Mylonakis E (2015) Modeling the 2014 Ebola virus epidemic–agent-based simulations, temporal analysis and future predictions for Liberia and sierra Leone. PLoS Curr 7

Siriprapaiwan S, Moore EJ, Koonprasert S (2018) Generalized reproduction numbers, sensitivity analysis and critical immunity levels of an Seqijr disease model with immunization and varying total population size. Math Comput Simul 146:70–89

Sobarzo A, Ochayon DE, Lutwama JJ, Balinandi S, Guttman O, Marks RS, Kuehne AI, Dye JM, Yavelsky V, Lewis EC et al (2013) Persistent immune responses after Ebola virus infection. N Engl J Med 369:492–493

Takaidza I, Makinde O, Okosun O (2017) Computational modelling and optimal control of Ebola virus disease with non-linear incidence rate. In Journal of Physics: Conference Series (p. 012003). IOP Publishing volume 818

Team WER (2014) Ebola virus disease in west Africa-the first 9 months of the epidemic and forward projections. N Engl J Med 371:1481–1495

Tiwari PK, Rai RK, Khajanchi S, Gupta RK, Misra AK (2021) Dynamics of coronavirus pandemic: effects of community awareness and global information campaigns. Eur Phys J Plus 136:994

Troncoso A (2015) Ebola outbreak in west Africa: a neglected tropical disease. Asian Pac J Trop Biomed 5:255–259

Tulu TW, Tian B, Wu Z (2017) Modeling the effect of quarantine and vaccination on Ebola disease. Adv Difference Equ 2017:1–14

Wang X-S, Zhong L (2015) Ebola outbreak in west Africa: real-time estimation and multiple-wave prediction. arXiv preprint arXiv:1503.06908

Wauquier N, Becquart P, Gasquet C, Leroy EM (2009) Immunoglobulin g in Ebola outbreak survivors, Gabon. Emerg Infect Dis 15:1136

Webb G, Browne C (2016) A model of the Ebola epidemics in west Africa incorporating age of infection. J Biol Dyn 10:18–30

Xia Z-Q, Wang S-F, Li S-L, Huang L-Y, Zhang W-Y, Sun G-Q, Gai Z-T, Jin Z (2015) Modeling the transmission dynamics of Ebola virus disease in Liberia. Sci Rep 5:1–13

Yang K-C, Hung H-F, Chen M-K, Chen SL-S, Fann JC-Y, Chiu SY-H, Yen AM-F, Huang K-C, Chen H-H, Wang S-T (2018) Cost-effectiveness analysis of universal influenza vaccination: application of the susceptible-infectious-complication-recovery model. Int J Infect Dis 73:102–108

Yusuf TT, Benyah F (2012) Optimal control of vaccination and treatment for an sir epidemiological model. World J Modell Simul 8:194–204

Zhang J, Qiao Y, Zhang Y (2022) Stability analysis and optimal control of Covid-19 with quarantine and media awareness. Math Biosci Eng 19:4911–4932

Zhang L, Addai E, Ackora-Prah J, Arthur YD, Asamoah JKK (2022b) Fractional-order Ebola-malaria coinfection model with a focus on detection and treatment rate. Comput Math Methods Med 2022

Publisher's Note Springer Nature remains neutral with regard to jurisdictional claims in published maps and institutional affiliations.

Springer Nature or its licensor (e.g. a society or other partner) holds exclusive rights to this article under a publishing agreement with the author(s) or other rightsholder(s); author self-archiving of the accepted manuscript version of this article is solely governed by the terms of such publishing agreement and applicable law.